

University at Albany, State University of New York

Scholars Archive

Chemistry

Honors College

5-2013

Charging and Self-Assembly of Fullerene Fragments

Michael V. Ferguson

University at Albany, State University of New York

Follow this and additional works at: https://scholarsarchive.library.albany.edu/honorscollege_chem

 Part of the [Chemistry Commons](#)

Recommended Citation

Ferguson, Michael V., "Charging and Self-Assembly of Fullerene Fragments" (2013). *Chemistry*. 4.
https://scholarsarchive.library.albany.edu/honorscollege_chem/4

This Honors Thesis is brought to you for free and open access by the Honors College at Scholars Archive. It has been accepted for inclusion in Chemistry by an authorized administrator of Scholars Archive. For more information, please contact scholarsarchive@albany.edu.

Charging and Self-Assembly of Fullerene Fragments

An honors thesis presented to the
Department of Chemistry
University at Albany, State University Of New York
In partial fulfillment of the requirements
for graduation with Honors in Chemistry with a Chemical Biology Emphasis
and
graduation from The Honors College.

Michael V. Ferguson

Research Advisor: Prof. Marina A. Petrukhina

April, 2013

I. Abstract

Buckybowls are bowl-shaped aromatic polycyclic hydrocarbons that map onto the surface of fullerene molecules, such as C_{60} and C_{70} , but lack their full closure. They are revered for their ability to undergo multiple reduction reactions, accepting several electrons, due to their degenerate and low energy LUMO orbitals.

Corannulene ($C_{20}H_{10}$), the smallest bucky bowl, is well known for its ability to accept up to four electrons. Many studies have been performed targeting preparation and characterization of corannulene anions using the NMR, ESR and UV-vis spectroscopic techniques. Corannulene has also been found to form a solid adduct with C_{60} without selectivity in its binding. Dibenzo[*a,g*]corannulene ($C_{28}H_{14}$), a larger π -bowl and focus of this work, contains a corannulene ring system with an addition of one peripheral benzene ring on each side. Originally studied as a synthetic precursor for creating carbon nanotube endcaps, $C_{28}H_{14}$ contains two consecutive low energy LUMO orbitals, making it also capable of accepting up to four electrons. Up until now, only NMR characterizations have been performed on $C_{28}H_{14}$ anions.

My research has resulted in the isolation of the first crystalline products of monoanion and dianion of $C_{28}H_{14}$ with alkali metal cations and their structural characterization using single crystal X-ray diffraction technique. Preference of metal binding to the *exo* surface of $C_{28}H_{14}$ has been revealed in the contact-ion pair of $[Rb(18\text{-crown-6})^+][C_{28}H_{14}^-]$. The first naked dianion of $C_{28}H_{14}$ was also isolated as its sodium salt, $[Na(18\text{-crown-6})(DME)^+]_2[Na_2(18\text{-crown-6})_2(DME)^{2+}][C_{28}H_{14}^{2-}]_2$, and characterized in this study. This allowed an evaluation of the bowl shape perturbation upon addition of one and two electrons. Both anions showed only small change in their bowl shape compared to neutral $C_{28}H_{14}$.

The supramolecular assembly of dibenzo[*a,g*]corannulene with fullerenes has been also investigated in this work by co-crystallization of $C_{28}H_{14}$ with C_{60} and C_{70} . Though packing of the $C_{28}H_{14}$ and C_{60} molecules paralleled that of $C_{20}H_{10}$ and C_{60} , a novel arrangement has been found for the solid-state structure of $C_{28}H_{14}$ and C_{70} . In the latter, selective binding of the *endo* surface of $C_{28}H_{14}$ to the *exo* surface of C_{70} was observed based on their perfect size and curvature complementarity.

II. Acknowledgements

I would like to express my earnest thanks and appreciation to my research advisor Dr. Marina A. Petrukhina for her amazing support and for allowing me to work in her lab over these past two years. I am grateful for the time and effort Dr. Petrukhina has spent revising and helping me grow as a scientist and writer. I appreciate the time and effort given to me by Dr. Alexander S. Filatov for his help with crystal structures determination and characterization. I would also like to thank the all of the members of our laboratory, past and present who have helped me grow as a chemist including Dr. Alexander V. Zabula, Dr. Oleksandr Hietsoi, Natalie J. Sumner, Michael Ihde. A special thank you to Cristina Dubceac for training me in our laboratory procedures during my first year in the laboratory, and to Sarah N. Spisak for her guidance in both my research and in the writing of my thesis.

I would also like to extend my gratitude to each of my roommates throughout these four years of college for helping me throughout my college experience. Thank you to Five Quad VAS for creating a second family for me here in Albany.

Lastly, I would like to thank my family and friends for their support of me throughout my life, especially my parents. They have constantly encouraged and challenged me throughout my life and have made me the person I am today; I am forever grateful for that.

Table of Contents

I. Abstract.....	2
II. Acknowledgments.....	3
III. Introduction.....	5
3. Fullerenes.....	5
3.1 Fullerene Fragments.....	6
3.1.1 Corannulene.....	6
3.1.1.1 Structure of Corannulene.....	7
3.1.1.2 Self-Assembly of Corannulene.....	9
3.1.1.3 Metal Coordination to Corannulene.....	13
3.1.1.4 Redox Properties of Corannulene.....	16
3.1.2 Dibenzo[<i>a,g</i>]corannulene.....	22
3.1.2.1 Synthesis of Dibenzo[<i>a,g</i>]corannulene.....	23
3.1.2.2 Solid State Structure of Dibenzo[<i>a,g</i>]corannulene.....	26
3.1.2.3 Redox Properties of Dibenzo[<i>a,g</i>]corannulene.....	27
IV. Results and Discussion.....	29
4.1 Co-crystallization of C ₂₈ H ₁₄ with Fullerenes.....	29
4.1.1 C ₂₈ H ₁₄ and C ₆₀	29
4.1.2 C ₂₈ H ₁₄ and C ₇₀	33
4.2 Characterization of Dibenzo[<i>a,g</i>]corannulene Anions.....	38
4.2.1 Rb Salt of C ₂₈ H ₁₄ Monoanion.....	38
4.2.2 Na Salt of C ₂₈ H ₁₄ Dianion.....	41
V. Experimental Part.....	43
5. Materials and Methods.....	43
5.1 Preparation of [C ₆₀ ·C ₂₈ H ₁₄] and [(C ₇₀)(C ₂₈ H ₁₄) ₂]·3C ₆ H ₄ Cl ₂	44
5.2 Preparation of [Rb(18-crown-6) ⁺][C ₂₈ H ₁₄ ⁻].....	45
5.3 Preparation of [Na(18-crown-6)(DME) ⁺] ₂ [Na ₂ (18-crown-6) ₂ (DME) ²⁺] [C ₂₈ H ₁₄ ²⁻] ₂	46
VI. Conclusions.....	47
VII. References.....	49

III. Introduction

3. Fullerenes

Fullerenes are a group of molecules that are becoming an increasing topic of study in the field of chemistry.^{1,2} They are an allotrope of carbon, like that of graphite and diamond, which conform to a very interesting structure. Similar to graphene, fullerenes contain alternating double and single carbon-carbon bonds. Fullerenes however, are capable of forming curved structures, such as spheres or ellipsoids, due to incorporation of both hexagonal and pentagonal carbon rings.³

The two most common examples of fullerenes are C_{60} and C_{70} (Figure 1); both of which are referred to as a buckyball.

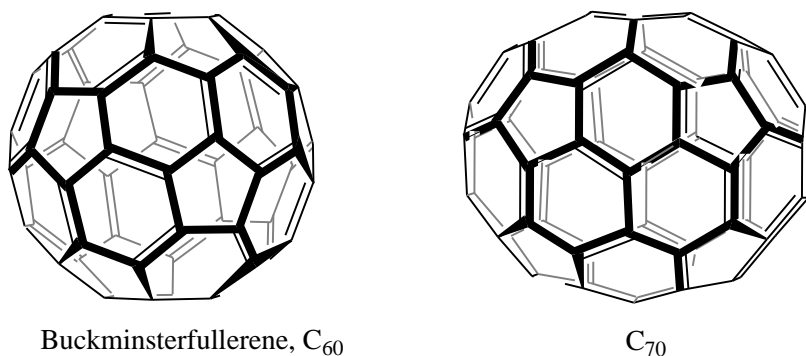


Figure 1. Schematic representation of the C_{60} (left) and C_{70} (right) fullerenes.

C_{60} consists of twenty hexagons and twelve pentagons, which are arranged in a spherical structure known as a truncated icosahedron. Another feature that makes C_{60} so interesting is the structure of its molecular orbitals.^{2,4} The LUMO of C_{60} is triply degenerate; this allows it to accept up to six electrons upon step-wise reduction.⁴ It should be mentioned, C_{60} is not superaromatic because it avoids having double bonds on

its pentagonal rings; hence C_{60} acts more as an alkene upon the formation of organometallic complexes.⁵ C_{70} is a fullerene consisting of twenty five hexagons and twelve pentagons that also has a degenerate set of LUMO orbitals; however it is only doubly degenerate.² This molecule can also accept six electrons upon reduction due to the fact that its LUMO +1 orbital is very close in energy to its LUMO orbital.² Due to both these remarkable electron accepting properties and the abundance of carbon in nature, fullerenes are currently being extensively studied to be potential electron acceptors to help create low cost organic solar cells and rechargeable batteries.^{6,7, 8}

3.1 Fullerene Fragments

3.1.1 Corannulene

Fullerene fragments are different molecules composed of carbon and hydrogen atoms whose carbon frameworks map onto the surface of fullerenes but lack their full closure. These curved polycyclic aromatic hydrocarbons are sometimes also referred to as buckybowls.^{9,10,11} One of the most studied buckybowls is dibenzo[ghi,mno]fluoranthene, also known as corannulene, $C_{20}H_{10}$ (Figure 2).

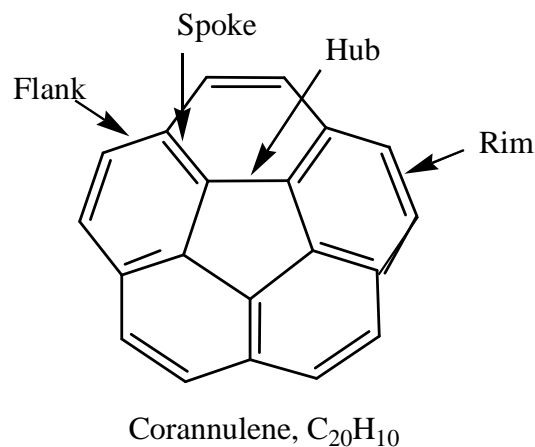


Figure 2. Schematic representation of corannulene.

Corannulene was first prepared by a tedious seventeen-step synthesis in 1966 by Barth and Lawton.¹² Corannulene remained largely unexplored until two decades later, when C_{60} was discovered by future Nobel Prize winners, Kroto, Heath, and Smalley.⁶ This prompted several organic chemistry groups to look for better preparation methods. Although corannulene is still not commercially available, alternate and more efficient methods have been developed since 1966, leading to an increased opportunity for exploration of this unique bucky bowl.^{7,13,14,15}

3.1.1.1 Structure of Corannulene

Corannulene is comprised of five hexagons that are fused to a central pentagon ring to form a bowl. Its bowl-shaped structure was first reported back in 1967 and was later re-evaluated at low temperature.¹⁶

There are four different types of C–C bonds that are found within corannulene (Figure 2). The shortened bond distances across the spoke and rim bonds suggest that

these are the locations of the double C–C bonds in the molecule (Table 1). It should be mentioned, the bowl depth of corannulene is 0.875(2) Å.¹⁶

Table 1. Key distances (in Å) for neutral C₂₀H₁₀.

	C ₂₀ H ₁₀ ^{16b}
hub	1.411(2)–1.417(2)
spoke	1.376(2)–1.381(2)
flank	1.441(2)–1.450(2)
rim	1.377(2)–1.387(2)
bowl depth	0.875(2)

The electrons in corannulene can delocalize putting six electrons around the central five-membered ring and fourteen electrons around its rim effectively creating an annulene-within-an-annulene (Figure 3).¹⁷ This in conjunction with its low energy, doubly degenerate LUMO allows corannulene to accept up to four electrons upon reduction.¹⁸

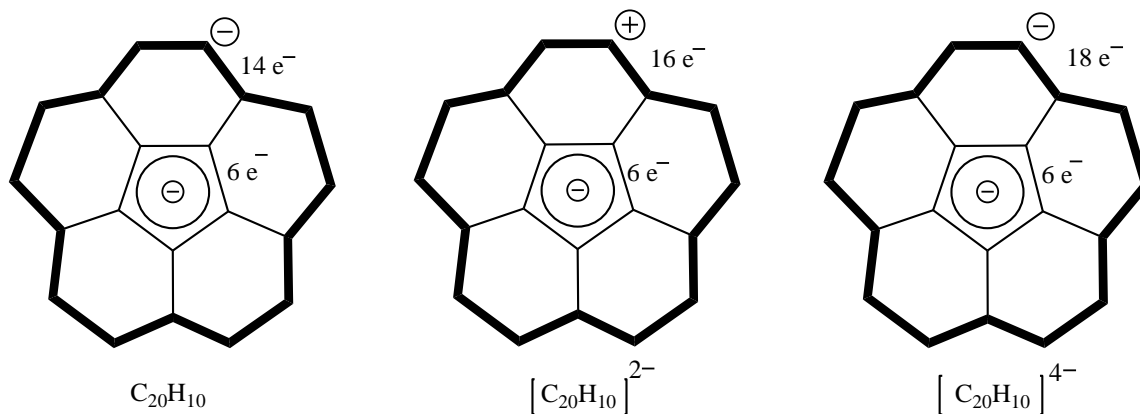


Figure 3. Annulene-within-an-annulene representation of $\text{C}_{20}\text{H}_{10}$, $[\text{C}_{20}\text{H}_{10}]^{2-}$, and $[\text{C}_{20}\text{H}_{10}]^{4-}$.

3.1.1.2 Self-Assembly of Corannulene

When packed together in the solid state, corannulene molecules associate with one another through two different types of intermolecular interactions. First is a $\pi \cdots \pi$ interaction between a convex and a concave facing molecule, forming a dimer (Figure 4).¹⁹ This interaction occurs through the centers of two 6-membered rings of the concave side of one molecule and the 6-membered ring on the convex face of the neighboring molecule. The second interaction places two of the dimers together to form a tetramer where two concave molecules interact through $\text{C-H} \cdots \pi$ bonding interactions from the two C-H bonds of a single 6-membered ring to the center of two 6-membered rings of the second molecule (Figure 5).^{16b, 20}

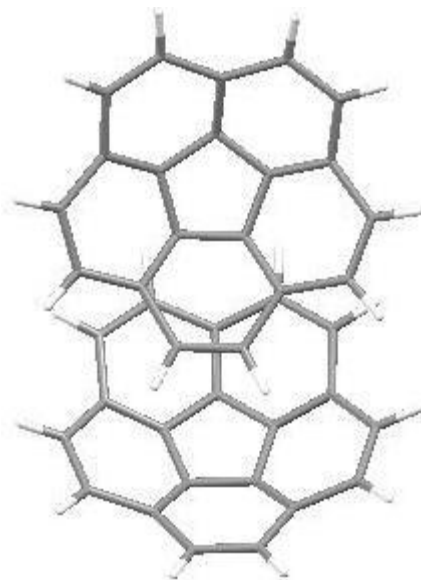


Figure 4. Top-view of the corannulene dimer showing the overlap of hexagonal rings.

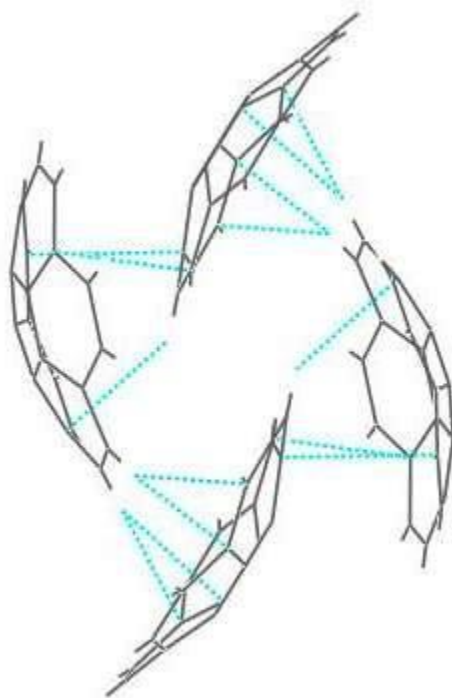


Figure 5. Side view of the corannulene tetramer showing the shortest contacts between the molecules.

It has been proposed for some time that the *endo* face of C₂₀H₁₀ is the ideal candidate for supramolecular binding to the electron-deficient surface of C₆₀. Although there are many theoretical investigations²⁰ that reveal the complexation of the *endo* surface of corannulene to C₆₀ is energetically favorable, the experimental proof was not revealed until very recently.²¹ The first X-ray structure of a stable C₆₀:C₂₀H₁₀ (1:1) adduct complemented the previous computational studies.²¹

According to an X-ray diffraction study, the C₆₀ molecules in the solid state structure of the C₆₀:C₂₀H₁₀ adduct pack in a zigzag manner with centroid–centroid contacts of 10.04 Å.²¹ Notably, this packing motif has been previously seen between C₆₀ molecules.²² The depth of penetration of the C₆₀ ball into corannulene is 6.94 Å (Figure 6). It should be mentioned, this is the distance from the centroid of the C₂₀H₁₀ five-membered ring to the centroid of the C₆₀ molecule. The shortest distance from the *endo* face of corannulene to C₆₀ is 3.06 Å (Figure 6). Contacts also exist from the convex face of corannulene to C₆₀; the shortest distance observed at 3.18 Å. There is no significant change in the geometry of corannulene upon co-crystallization with C₆₀. The bowl depth of corannulene in C₆₀:C₂₀H₁₀ is 0.89 Å, compared to 0.88 Å in the parent ligand.

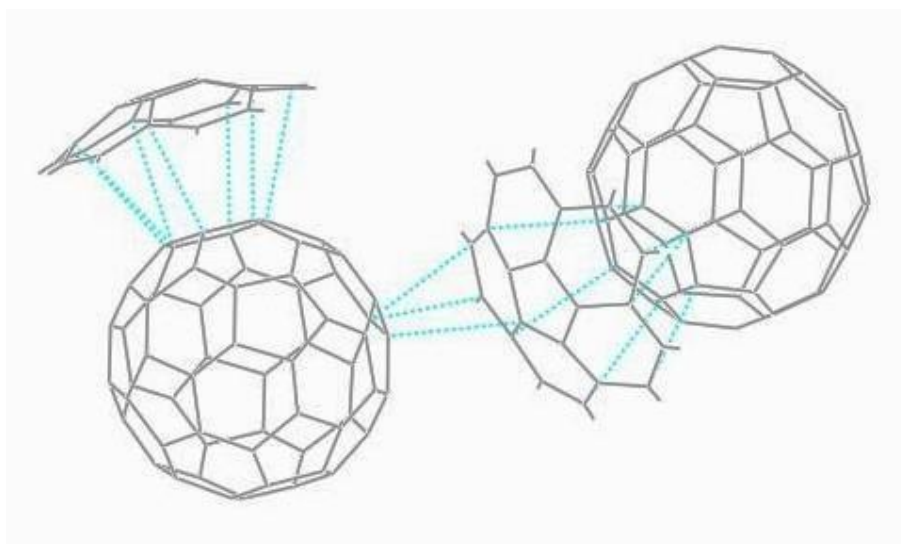


Figure 6. Three dimensional view of the packing of C_{60} and $C_{20}H_{10}$ showing the *endo* and *exo*-binding of corannulene to C_{60} .

Due to a good size match between the concave surface of $C_{20}H_{10}$ and convex surface of C_{60} it was theorized that C_{60} would be able to interact with receptor $C_{20}H_{10}$ molecules in a “ball and socket” fashion through $\pi \cdots \pi$ interactions. In 2007, Sygula showed this was possible after creating a pair of “molecular tweezers” with the composition of $C_{60}H_{24}$ from two corannulene-based subunits (Figure 7).²³ In this structure, fullerene is observed sitting between two concave faces of corannulene pincers; the depth of penetration of C_{60} into each corannulene subunit is 6.77 Å. This is noticeably shorter than the free packing of $C_{20}H_{10}$ and C_{60} and most likely due to C_{60} having to interact with the corannulene subunits within the rigid structure of the “tweezers”. The application that stems from this work is to use fullerenes as guests and corannulene as a selective receptor in supramolecular chemistry.

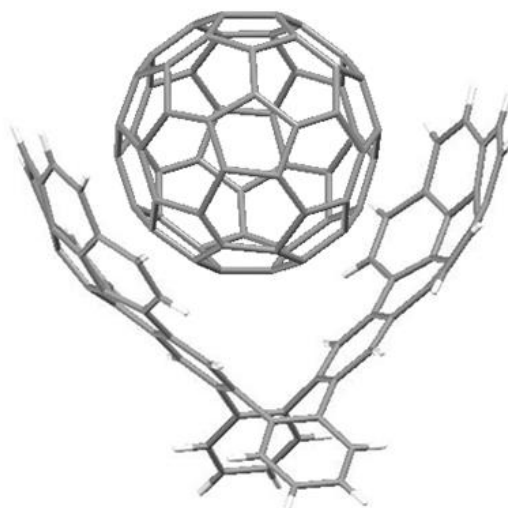


Figure 7. C₆₀ coordinated to the corannulene subunits of molecular tweezers.

3.1.1.3 Metal Coordination to Corannulene

Corannulene is a unique and intriguing π -ligand, which provides interior and edge carbon atoms for binding, along with concave and convex unsaturated carbon surfaces (Figure 8).²⁴

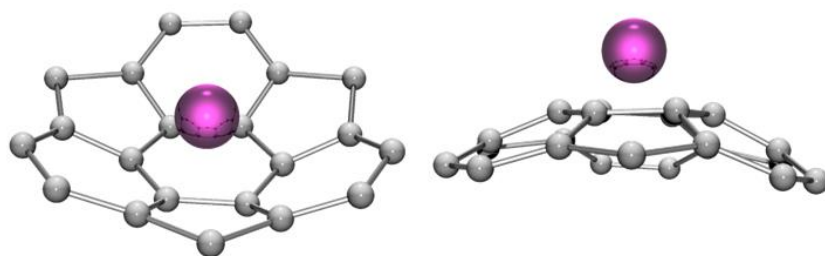


Figure 8. Coordination possibilities of buckybowls: *endo* (left) and *exo* (right).

Complexes of transition metals with curved polyaromatic hydrocarbons have attracted substantial interest in recent years due to their fundamental and practical

importance. As mentioned previously, buckybowls, such as corannulene, are exceptional ligands with multiple binding sites.²⁵ X-ray diffraction studies have indicated the strong preference of convex metal coordination in all discrete complexes having a single metal bound to C₂₀H₁₀ in an η^6 -fashion, such as in $[(\eta^6\text{-C}_6\text{Me}_6)\text{Ru}(\eta^6\text{-C}_{20}\text{H}_{10})][\text{PF}_6]_2$.²⁶

Our group has been extensively involved in studying the coordination preferences of corannulene.²⁴ Back in 2003, the first complexes with $[\text{Rh}_2(\text{O}_2\text{CCF}_3)_4]$ were isolated and structurally characterized,²⁷ followed by crystallization of $[\text{Ru}_2(\text{O}_2\text{CCF}_3)_2(\text{CO})_4 \cdot (\eta^2\text{-C}_{20}\text{H}_{10})_2]$ (Figure 9) in 2006.²⁸ All these complexes showed the preference for *exo*-metal binding to the rim sites of corannulene.

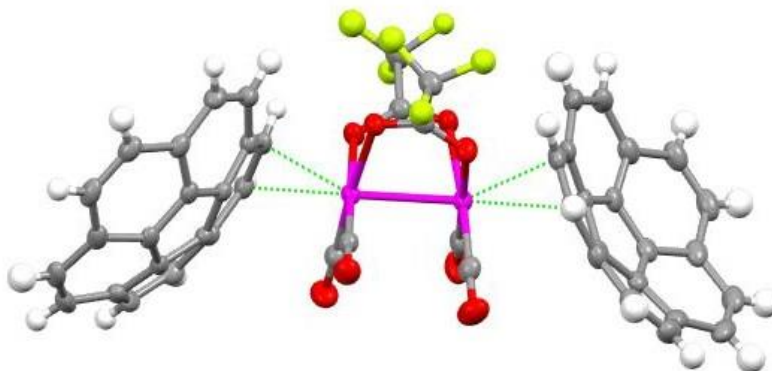
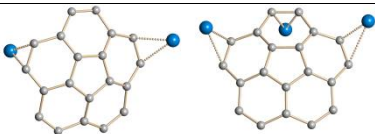
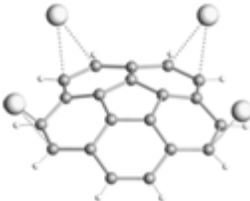
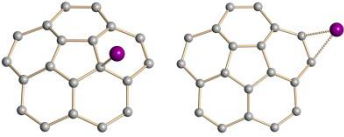
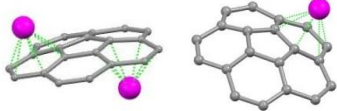


Figure 9. Molecular structure of $[\text{Ru}_2(\text{O}_2\text{CCF}_3)_2(\text{CO})_4 \cdot (\eta^2\text{-C}_{20}\text{H}_{10})_2]$.

Preferential binding of the above metal centers to rim C–C bonds led our group to search for less electrophilic metal units for buckybowl binding. Then again in 2006, two new ruthenium(I) complexes were crystallized within the same crystal of $[\text{Ru}_2\{\text{O}_2\text{C}(3,5\text{-CF}_3)_2\text{C}_6\text{H}_3\}_2 \cdot (\text{CO})_5] \cdot (\frac{1}{4} \text{C}_{20}\text{H}_{10})$.²⁹ One of the complexes showed Ru(I) binding to the rim of C₂₀H₁₀, while the other had the Ru(I) center bound to the hub bonds of C₂₀H₁₀. In

both of these complexes however, Ru(I) was bound to the *exo* surface of C₂₀H₁₀, further exemplifying the convex preference of transition metal binding to C₂₀H₁₀. Until 2011, only discrete *exo* or multi-coordinated C₂₀H₁₀ with metals were known. *Endo* coordination was noticed in multi-coordinated C₂₀H₁₀, however these contained *exo* bound metals as well so it was not clear what is the primary coordination mode and what is the result of packing (Table 2).

Table 2. Coordination modes of various metals with C₂₀H₁₀ with hydrogen atoms omitted for clarity.

Formula	Coordination modes	
C ₂₀ H ₁₀		$\mu_2\text{-}\eta^2\text{:}\eta^2\text{-rim}^{30}$ $\mu_3\text{-}\eta^2\text{:}\eta^2\text{:}\eta^2\text{-rim}^{10}$
		$\mu_4\text{-}\eta^2\text{:}\eta^2\text{:}\eta^2\text{:}\eta^1\text{-rim}^{30}$
		$\eta^1\text{-exo-hub}^{29}$ $\eta^2\text{-exo-rim}^{28}$
		$\mu_2\text{-}\eta^6\text{:}\eta^6^{31}$ $\eta^6\text{-exo}^{26,32}$

Despite all prior examples of the preferential coordination of transition metal centers to the *exo* surface of corannulene, the inside *endo* face can also be engaged in metal coordination. In our laboratory, we have recently revealed the unprecedented selective *endo*-binding of a metal to the monoreduced corannulene bowl (Figure 10). Single crystals of $[\text{Cs}(\text{18-crown-6})]^+[\text{C}_{20}\text{H}_{10}]^-$ were grown from a diglyme solution by layering it with hexanes.³³

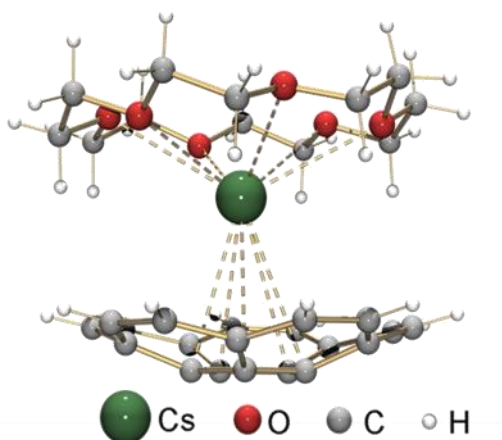


Figure 10. Molecular structure of $[\text{Cs}(\text{18-crown-6})]^+[\text{C}_{20}\text{H}_{10}]^-$.

The cesium cation, bearing 18-crown-6, sits almost exactly above the center of the five-membered ring, representing the first example of η^5 -binding of a metal center to the corannulene moiety. This and other examples illustrate that corannulene can function in a variety of binding modes towards various metal centers.

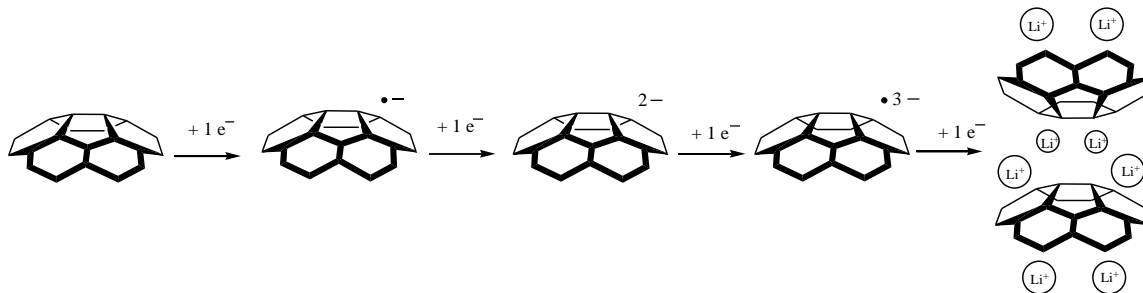
3.1.1.4 Redox Properties of Corannulene

Corannulene can accept up to four electrons due to its doubly-degenerate and low-lying LUMO. The first *in-situ* observation of the corannulene anion was in 1967 soon

after the preparation of corannulene.¹³ In 1994, Scott found, upon reduction with lithium, corannulene was able to be reduced to a tetraanion.^{18b} In 1995, Scott and coworkers were able to characterize each of the four reduction stages of corannulene (Scheme 1) when reacted with lithium through the use of UV-Vis spectroscopy and ¹H nuclear magnetic resonance spectroscopy (NMR).³⁴

The first reduction stage was noticed with a change in color in the solution to green (monoanion). This was characterized through a collection of optical absorption data, which found maxima at the following wavelengths in THF-*d*₈: 443, 648, 805, and 904 nm.³⁴ The next reduction stage was found with a color change to purple (dianion) and a new maximum at 503 nm. This stage was also accompanied by a shift in the ¹H NMR signal to −5.6 ppm, implying that the dianion has a paratropic ring current.³⁴ This suggests it has a delocalized 16-electron perimeter annulene that gives it the antiaromatic and thus paratropic character (Figure 3). Recently, the corannulene trianion was found with another shift in the optical absorption spectra to a maximum of 386 nm in diglyme and a lack of ¹H NMR due to peak broadening.³⁵ The final stage of the reduction, the tetraanion, was found with a change of color to brown and a shift in its optical absorption spectrum to maxima located at 460, 605, and 714 nm in diglyme.³⁶ This was characterized by the return of the ¹H NMR spectra again and shift of 6.92 ppm, suggesting the return of the aromatic character of the perimeter annulene ring as well as the diatropic character of the molecule (Figure 3).

Scheme 1



The corannulene anions, ranging from monoanion to tetraanion, have been detected in solution; however, their solid-state products were not isolated in the single crystalline form until very recently, due to their extreme sensitivity to air and moisture.³⁷ In our group, the first “naked” monoanions were found with alkali metals, Li^+ , Na^+ , and Rb^+ when solvents or crown ethers provide full encapsulation of the metal center (Figure 11).^{33,38} When the coordination sphere of the alkali metals is incomplete, different binding modes can be seen in the solid-state products. Throughout our work, the general trend we have observed has been lighter alkali metals, such as lithium and sodium often form solvent-separated products (SSIP) with “naked” $\text{C}_{20}\text{H}_{10}^{\bullet-}$; whereas, heavier alkali metals tend to bind to the surface of the corannulene monoanion. Cesium, the largest alkali metal, shows preferential *endo* binding to the curved carbon surface.³³

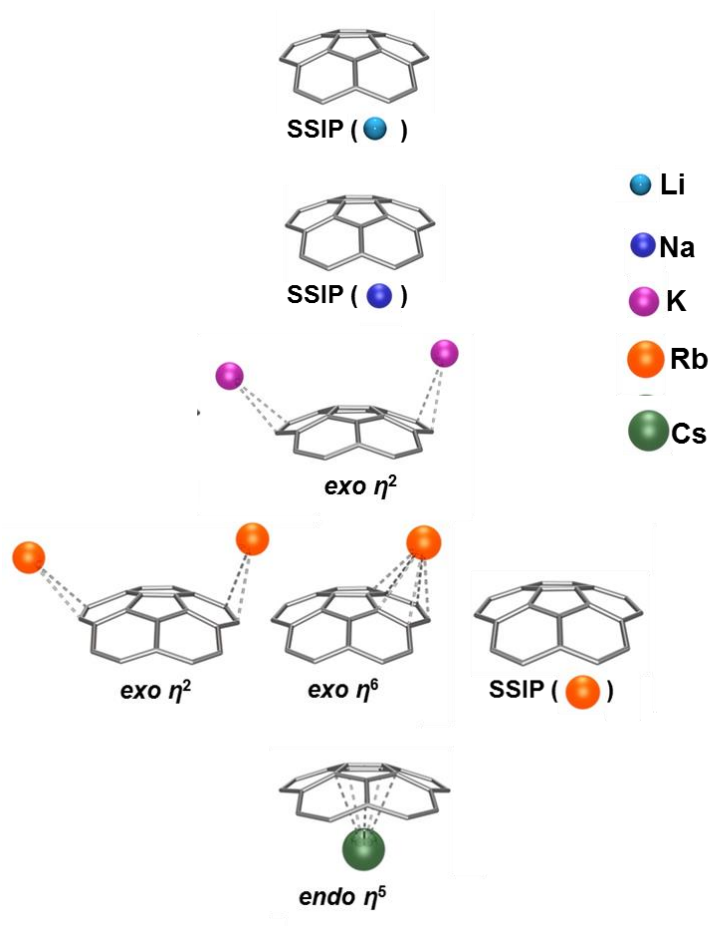


Figure 11. Structural representation of corannulene monoanions with alkali metal ions.

This work has recently been extended to the second reduction stage of corannulene. We have selectively prepared the $C_{20}H_{10}^{2-}$ anions with the series of Group 1 metals, Li, Na, K, and Cs (Figure 12).^{38, 39} These products have been characterized by single crystal X-ray diffraction and spectroscopic techniques. The first “naked” corannulene dianion has been found with the lightest alkali metal, lithium; whereas, heavier alkali metals tend to form contact-ion pairs (CIP). It was observed that the bowl depth of corannulene dianions is much greater than the calculated value of 0.57 Å, confirming the importance of experimental structural studies.⁴⁰

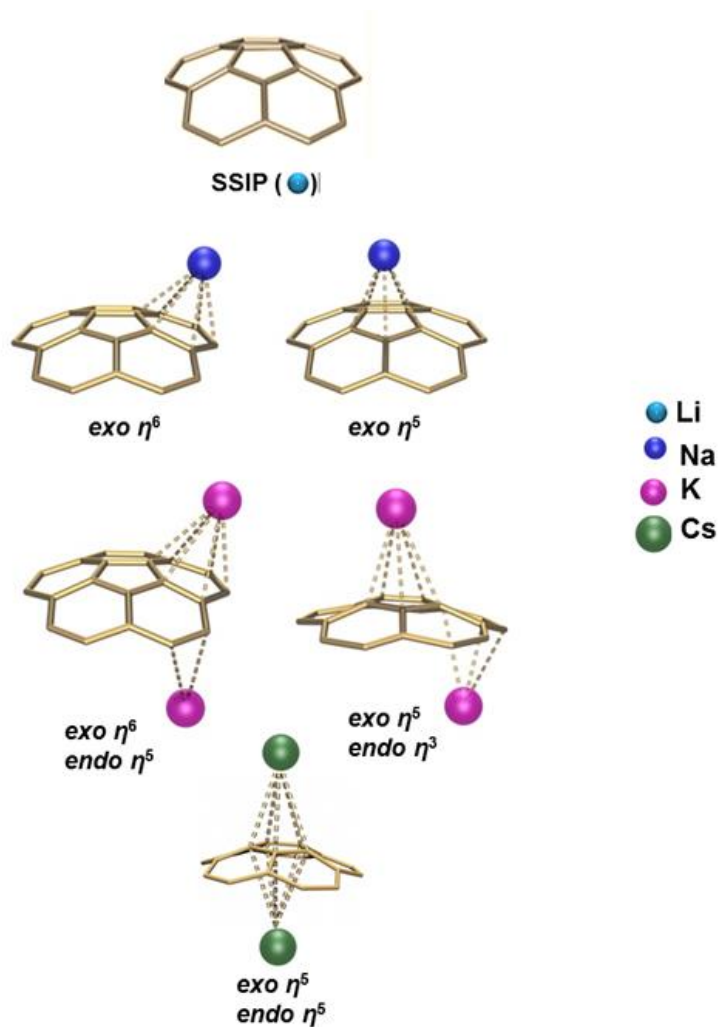


Figure 12. Structural representation of the corannulene dianions with alkali metal ions.

Based on earlier NMR studies, investigators concluded that the tetraanions of corannulene aggregate into supramolecular dimers charge-compensated by coordinated lithium ions.¹⁸ Two tetraanions in the dimer were described as “glued” together by four lithium ions to form a “stable high-order molecular sandwich” in solution (Figure 13)

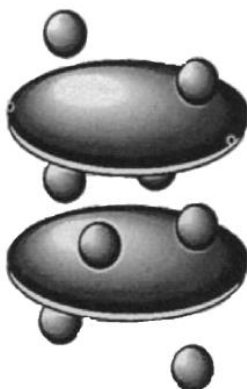


Figure 13. Formal representation of corannulene tetraanions (disks) and eight lithium cations (balls) in a dimer.

The residual four lithium ions were suggested to bind to the dimer exterior: two on the top and two on the bottom of the sandwich. Although the original NMR data were inconclusive about the location of the lithium ions and the depths and relative orientations of the two bowls, this proposed model has been largely accepted as the model for the assembly of reduced buckybowls with lithium ions ever since.^{18b}

Since direct structural characterization of the resulting self-assembled product was missing, our laboratory had focused on the crystallization of this fascinating product. After multiple attempts, the lithium salt of $C_{20}H_{10}^{4-}$ was crystallized by the slow diffusion of hexanes vapors into a THF solution of the product kept at 15 °C. In contrast to the previously proposed model,^{18b} five lithium ions were found sandwiched between the two anionic corannulene decks in the solid-state (Figure 14).^{36,37} Two more lithium ions are bound to the external surface of this supercharged sandwich, one on the top and on the bottom, while the remaining lithium cation is solvent-separated. The overall product can be written as $[Li(THF)_4]^+ \{ [Li(THF)_2] // [Li_5(C_{20}H_{10})_2] // [Li(THF)_3] \}^-$

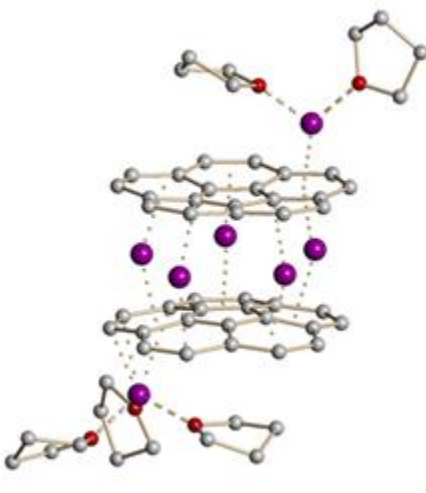


Figure 14. Structural representation of the $C_{20}H_{10}$ tetraanion sandwich compound.

The above work revealed a novel model of lithium intercalation between highly charged corannulene bowls. In contrast to corannulene, these studies have yet to be accomplished for larger buckybowls.

3.1.2 Dibenzo[*a,g*]corannulene

Another fullerene fragment that maps onto the surface of C_{60} is dibenzo[*a,g*]corannulene, $C_{28}H_{14}$ (Figure 15). Fundamental interest in this molecule stems from the idea that it may be used in the synthesis of specific carbon nanotube endcaps.⁴¹ There are three types of carbon nanotubes that are known to form, namely arm-chair, zig-zag, and chiral.⁴² Each type has its own physical and electronic properties that are interesting to researchers. Scientists are looking to synthesize particular nanotubes by building and extending the endcap specific to that nanotube. Scott *et al.*

found that it was possible to create the endcap for an arm-chair carbon nanotube using dibenzo[a,g]corannulene as the starting reagent.⁴³

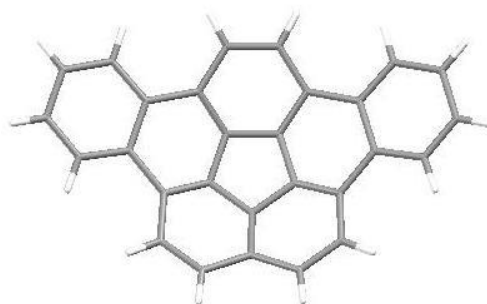
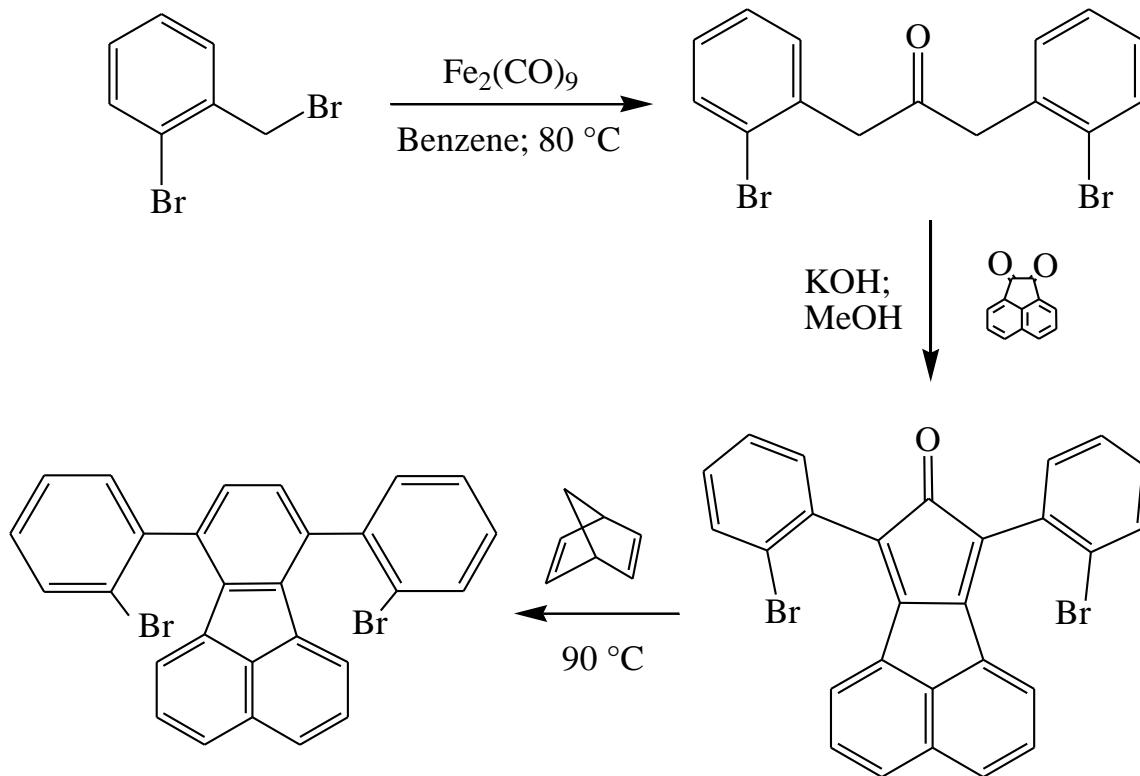


Figure 15. Structure of dibenzo[a,g]corannulene.

3.1.2.1 Synthesis of Dibenzo[a,g]corannulene

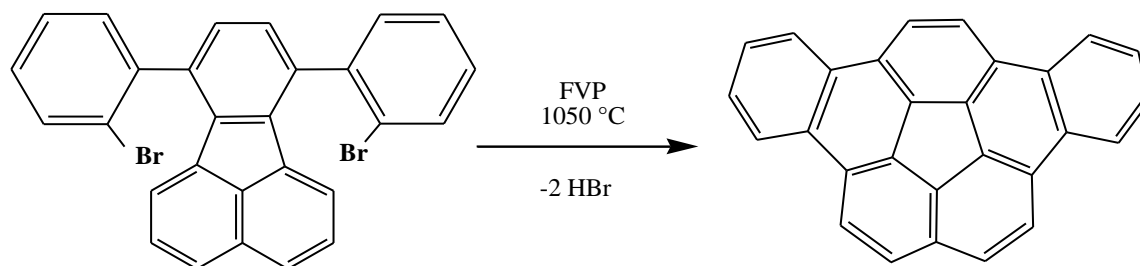
The first synthesis of $C_{28}H_{14}$ was accomplished in 1994 by the group of Scott.⁴⁴ In order to prepare, dibenzo[a,g]corannulene, its precursor 10-di(2-bromophenyl)fluoranthene must be synthesized (Scheme 2).⁴⁵ To make this molecule, 2-bromobenzyl bromide and diironnonacarbonyl are placed in anhydrous benzene and refluxed forming 1,3-di(2-bromophenyl)acetone. Next, 1,3-di(2-bromophenyl)acetone is mixed with acenapthequinone in a basic solution to form 7,9-bis(2-bromophenyl)-8H-cyclopenta[a]acenapthylen-8-one. Lastly, the 7,9-bis(2-bromophenyl)-8H-cyclopenta[a]acenapthylen-8-one is refluxed with 2,5-norbornadiene in a pressure flask in order to form 10-di(2-bromophenyl)fluoranthene. This same procedure has also been used to convert 2-chlorobenzyl chloride into 10-di(2-chlorophenyl)fluoranthene.

Scheme 2.



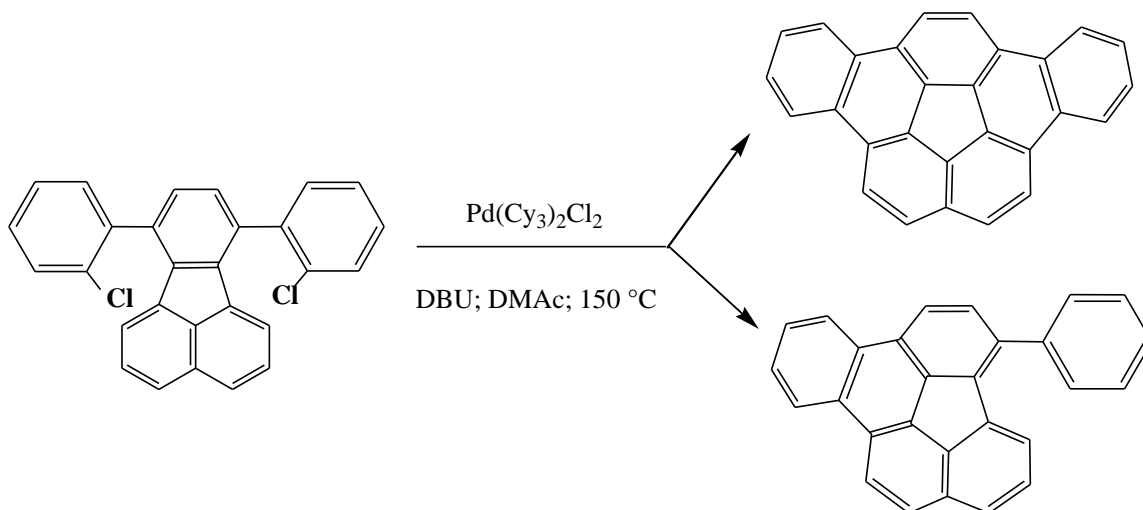
The original synthetic method of creating $\text{C}_{28}\text{H}_{14}$ was based on the use of flash vacuum pyrolysis (FVP) to break the aryl-halide bonds in 10-di(2-bromophenyl)fluoranthene and move the 2-bromophenyl units within bonding distances to form curved ring systems. Though the FVP method of creating $\text{C}_{28}\text{H}_{14}$ is useful, it requires very high temperatures over 1000°C (Scheme 3). The reaction scale is also restricted to about 1-2 g with about 15-30% yields. Notably, yields of the brominated precursor are greater than that of the chlorinated precursor.

Scheme 3.



Due to the above limitations, Scott's group looked into a solution-based way of producing $C_{28}H_{14}$. Their first look was the palladium catalyzed aryl-aryl coupling reactions. These reactions use the elimination of HX in the arylation. This method, while being successful, also resulted in the formation of a byproduct known as idenochrysene, which stems from reductive bromination occurring on one side of the molecule. The results for the brominated precursor were optimized using Herrmann's palladacycle, 1,8-diazabicyclo[5.4.0]undec-7-ene (DBU), and N,N-dimethylformamide (DMF) at 150 °C for 72 hours. It was also found that the use of the chlorinated precursor provided a greater product yield, improving the ratio of product:byproduct from 3:1 with the brominated precursor to 10:1 with the chlorinated one.⁴¹ Slight improvements were made to this procedure by substituting Herrmann's palladacycle with $Pd(PCy_3)_2Cl_2$ and DMF with anhydrous DMAc, which is the currently used procedure (Scheme 4).⁴¹ In our work, we utilized this preparation scheme, accommodating all the latest improvements. We have improved further on the product purity by additional washing of the final product with hexanes followed by acetone.

Scheme 4.



3.1.2.2 Solid State Structure of Dibenzo[*a,g*]corannulene

The solid state structure of $\text{C}_{28}\text{H}_{14}$ was elucidated in our group back in 2005.⁴⁶ When packed together, $\text{C}_{28}\text{H}_{14}$ molecules associate with one another in a much different way than corannulene. The addition of two benzene rings to the core of corannulene causes the shape of the bowl in $\text{C}_{28}\text{H}_{14}$ to widen, resulting in a shallower bowl depth: $0.830(3) \text{ \AA}$ vs. $0.875(2) \text{ \AA}$ in corannulene. This change in shape as well as the addition of the two benzene rings is believed to be what causes the difference in packing in $\text{C}_{28}\text{H}_{14}$.⁴³ In the solid state, $\text{C}_{28}\text{H}_{14}$ bowls form 1D columnar stacks, in which the molecules are staggered so that the outer benzene rings of $\text{C}_{28}\text{H}_{14}$ line up with the central corannulene core of the next molecule (Figure 16). This is believed to maximize the $\pi\cdots\pi$ stacking interactions between the bowls.⁴⁶ Moreover, the peripheral benzene rings have a much lower negative potential than the five-membered core so it is electrostatically favorable that they line up with the five-membered cores being as far apart as possible. The resulting 1D stacks are also able to interact with one another using $\text{C-H}\cdots\pi$ bonding

between the free peripheral benzene and one of the six-membered core rings in an adjacent stack (Figure 11).¹⁹

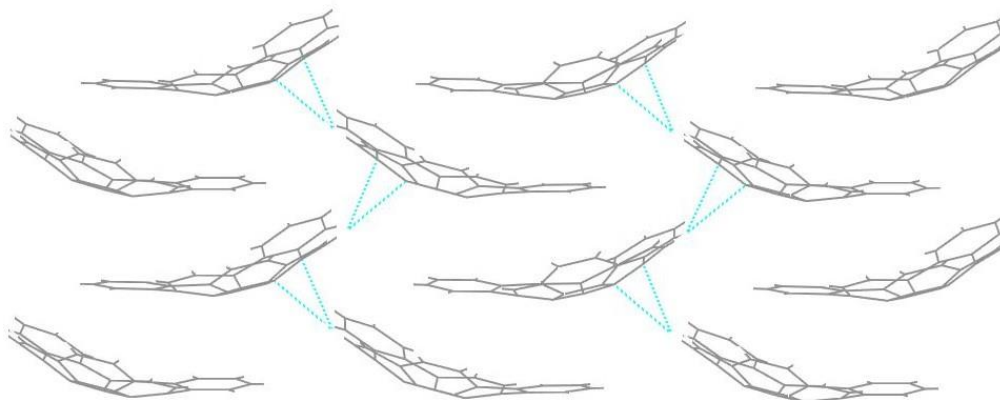


Figure 16. The two-dimensional packing of $C_{28}H_{14}$ from a side view showing the shortest contacts between adjacent stacks.

3.1.2.3 Redox Properties of Dibenzo[*a,g*]corannulene

Like corannulene, $C_{28}H_{14}$ can accept and delocalize multiple electrons.⁴⁷ Though its LUMO orbital is not doubly degenerate, the two lowest LUMO orbitals are close in energy, theoretically allowing $C_{28}H_{14}$ to accept up to four electrons upon step-wise reduction.^{47a}

In 1998, Scott reduced $C_{28}H_{14}$ using lithium and potassium metals. With lithium, he noticed that $C_{28}H_{14}$ underwent a maximum of three reduction states. The first led to a change of color to green, resembling that of a corannulene monoanion, which is also supplemented with the loss of an NMR spectrum, consistent with the formation of a monoanion-radical. The second reduction of $C_{28}H_{14}$ came with a color change to purple and a return of NMR spectra. The upfield shifts of protons of $C_{28}H_{14}$ came to resemble

that of the paratropic corannulene dianion with slight dampening, an effect thought to be due to quenching from the attached benzene rings (Figure 17).

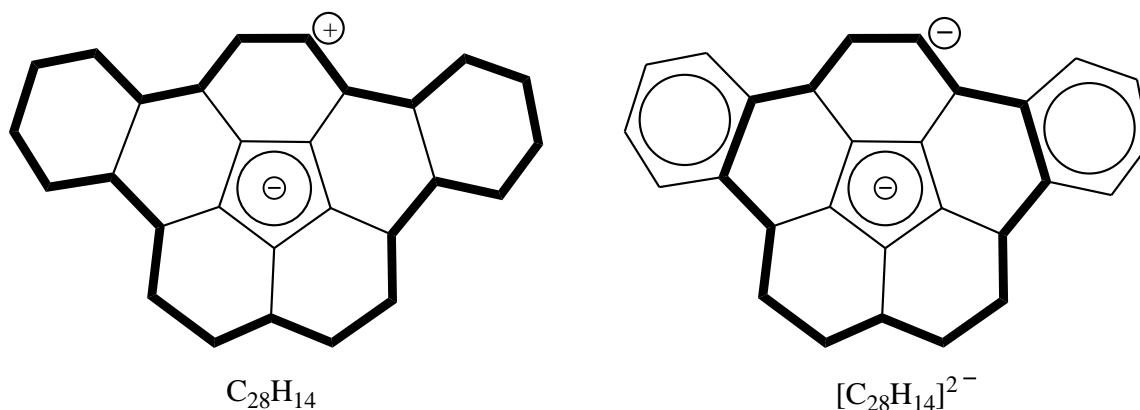


Figure 17. Schematic representations of the superaromatic structures of $C_{28}H_{14}$ and $[C_{28}H_{14}]^{2-}$.

$C_{28}H_{14}$ can be readily reduced to the dianion stage with lithium metal.⁴⁷ However, after extended time, slow disappearance of the NMR spectrum may suggest the formation of radical trianions. For potassium, the first three reduction stages showed very similar results. However, in addition, a fourth stage was noticed with a color change from purple to brown, and the return of a NMR spectrum. This new 1H NMR spectrum however was different from the $C_{28}H_{14}$ dianion. It exhibited much broader peaks as well as a larger downfield shift suggesting the return of the diatropic character as seen in the neutral molecule. It is theorized that the further reduction is due in part to the use of a stronger reducing metal, potassium, which is able to bind more tightly to the anion in solution.⁴⁷ So far the reduction reactions of $C_{28}H_{14}$ have been investigated only in situ using spectroscopic methods. None of the products have been isolated in the solid state.

Therefore the effects of adding multiple electrons to this bowl core have not been evaluated. In this work, we have targeted isolation of the first crystalline solid products of the reduced dibenzo[*a,g*]corannulene bowl (Part 4.2). We have also investigated self-assembly of C₆₀ and C₇₀ fullerenes with C₂₈H₁₄ (Part 4.1) and compared that with the corannulene adducts.

IV. Results and Discussion

4.1 Co-crystallization of C₂₈H₁₄ with Fullerenes

4.1.1 C₂₈H₁₄ and C₆₀

Since no differentiation between the concave-convex and convex-convex binding was observed in the solid structure of the C₂₀H₁₀-C₆₀ adduct,²¹ in this work we set to investigate if C₂₈H₁₄ is a better host for fullerene guests. Single crystals of the product were obtained by the slow evaporation of the chlorobenzene (C₆H₅Cl) solution containing C₆₀ and C₂₈H₁₄ (1:1) in a sealed ampoule over 5 days. The X-ray crystallographic study confirmed the formation of the product having a 1: 1 composition of C₂₈H₁₄ to C₆₀ (**1**). Analysis of the structure shows the *endo* face of the C₂₈H₁₄ molecule is interacting with the convex C₆₀ molecule (Figure 18).

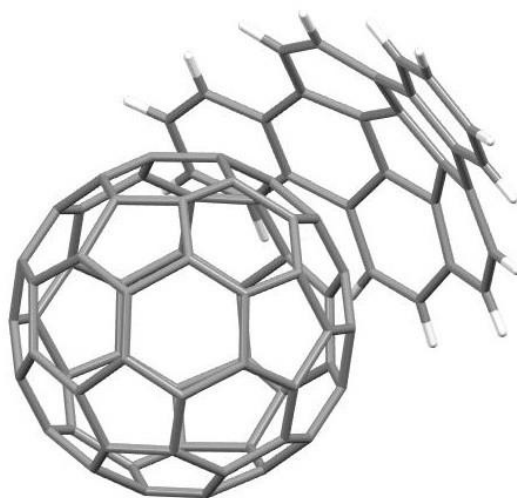


Figure 18. Molecular structure showing a formation of an inclusion complex of C_{60} and $C_{28}H_{14}$ in a 1:1 ratio.

The depth of penetration of the C_{60} ball into the $C_{28}H_{14}$ bowl is 6.71 Å, measured from the centroid of the $C_{28}H_{14}$ five-membered ring to the centroid of C_{60} , and 3.137(3) Å, measured from the shortest distance from the concave surface of the $C_{28}H_{14}$ to a C_{60} surface. A notable difference is observed in the increased length of the spoke and flank bonds of $C_{28}H_{14}$.⁴⁶ However, the bowl depth of dibenzo[a,g]corannulene in **1** is similar to that observed in $C_{28}H_{14}$ (Table 2).

Table 2. Key distances of **1** and **2** (Å).

	C₂₈H₁₄ ⁴⁶	1	2
hub	1.4208(2)–1.428(2)	1.4157(1)–1.4273(1)	1.404(1)–1.431(2) 1.410(1)–1.429(2)
rim	1.385(2)–1.447(2)	1.3760(1)–1.4431(1)	1.378(1)–1.448(2) 1.382(1)–1.439(2)
spoke	1.367(2)–1.380(2)	1.3680(1)–1.4732(1)	1.362(1)–1.377(2) 1.367(1)–1.382(2)
flank	1.435(2)–1.472(2)	1.4317(1)–1.4862(1)	1.418(1)–1.481(1) 1.426(2)–1.476(1)
peripheral rings	1.382(2)–1.407(2)	1.3641(1)–1.4096(1)	1.372(1)–1.405(1) 1.373(2)–1.413(1)
bowl depth	0.83	0.802	0.790 0.796

After expanding the asymmetrical unit, it was noticed that the C₆₀ molecules in **1** pack in a zig-zag manner just as they did in the C₂₀H₁₀:C₆₀ crystals (Figure19).²¹ The distance between consecutive C₆₀ molecules is 13.13 Å and the angle between three successive molecules is 142.81°. The C₂₈H₁₄ molecules along the row interact with C₆₀ through convex-convex $\pi \cdots \pi$ interactions with the shortest distance being 3.2207(2) Å.

The formation of a 2D structure was observed with the anti-parallel aligning of the neighboring 1D strands (Figure 19). These strands exhibit $\pi \cdots \pi$ interactions between neighboring C₆₀ molecules, with the shortest distance being 3.074(2) Å. An extended structure is formed by the translation of these strands forming a sheet. Three different interactions were observed within this network. The first exists as $\pi \cdots \pi$ interactions between the *exo* faces of adjacent C₂₈H₁₄ molecules at a distance of 3.2485(3) Å. The

second, a C–H \cdots π interaction, is also found between these faces at a distance of 2.8009(3) Å. The last is a C–H \cdots π between the peripheral ring of C₂₈H₁₄ and C₆₀ at a distance of 2.5723(2) Å.

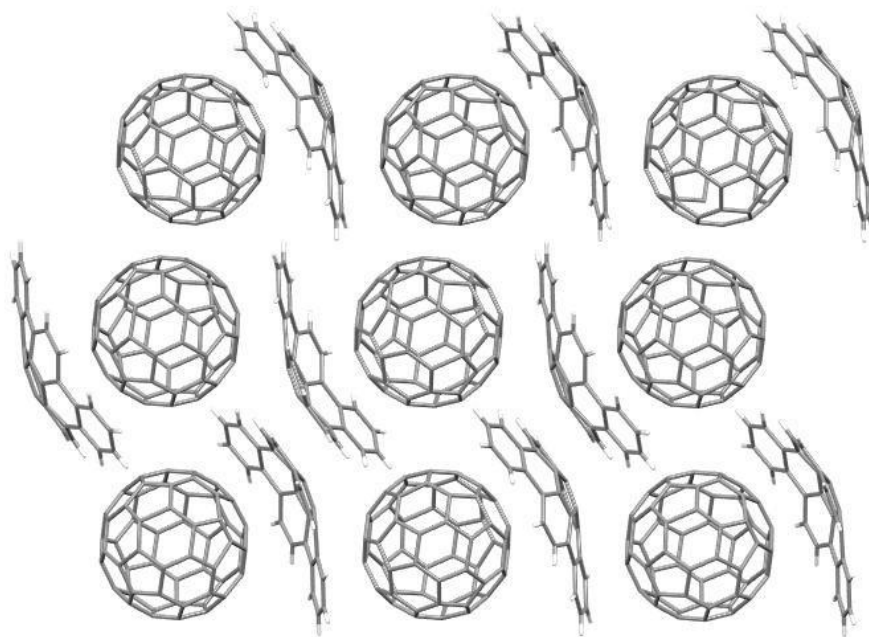


Figure 19. A 2D representation of **1** with C₆H₅Cl omitted for clarity.

Through expansion of these sheets along the *b* crystallographic axis, a 3D structure is formed for the crystal (Figure 20). The sheets appear to be held together by the $\pi\cdots\pi$ interactions between neighboring C₆₀ molecules; the shortest distance observed at 3.277(3) Å. A C–H \cdots π interaction also exists between C₂₈H₁₄ and C₆₀, adding extra connectivity and supporting growth in the third dimension.

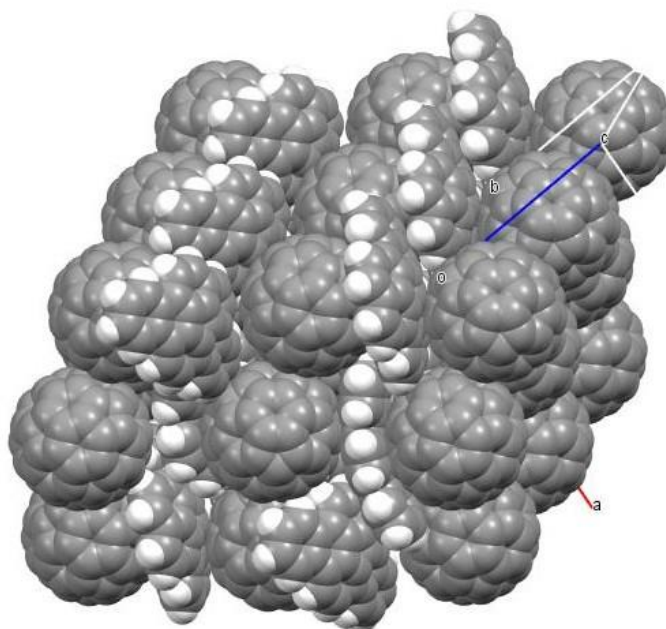


Figure 20. Space-filling model of the 3D structure of **1**.

4.1.2 C₂₈H₁₄ and C₇₀

Single crystals of the product were obtained by slow evaporation of the 1,2-dichlorobenzene (DCB) solution containing C₇₀ and C₂₈H₁₄ (1:1) in a sealed ampoule over 5 days. The X-ray crystallographic study confirmed the formation of the product having a composition of [(C₇₀)(C₂₈H₁₄)₂] \cdot 3C₆H₄Cl₂ (**2**).

Analysis of the structure reveals the formation of a unique self-assembly in which the *endo* face of two C₂₈H₁₄ molecules embraces the C₇₀ spheroid along its elongated major axis (Figure 21). This could be expected because unlike C₆₀, which provides a uniform ball surface for C₂₈H₁₄ to interact with, C₇₀ exhibits two distinctly different surfaces along the minor and major axes. This selective interaction between C₇₀ and

$C_{28}H_{14}$ is very interesting and most likely due to the decreased bowl depth of $C_{28}H_{14}$, providing a perfect complementary surface and curvature match towards C_{70} .

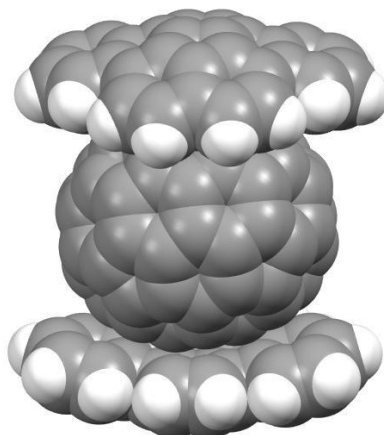


Figure 21. Molecular structure showing the encapsulation of C_{70} between two $C_{28}H_{14}$ units.

The depth of penetration of C_{70} into the closer $C_{28}H_{14}$ bowl is 6.95 Å, measured from the centroid of the bowl five-membered ring to the centroid of the C_{70} molecule, and 3.258(1) Å, measured from the shortest distance from the concave surface of the $C_{28}H_{14}$ to a C_{70} surface. The other independent $C_{28}H_{14}$ molecule has very similar distances with a penetration of 7.00 Å measured to the centroid of C_{70} , and 3.267(1) Å as its shortest contact to the C_{70} surface (Figure 21). The hub C–C bond lengths of $C_{28}H_{14}$ in **2** are notably shorter than in the parent ligand.⁴⁶ The bowl depth of dibenzo[*a,g*]corannulene in **2** is similar to that observed in the $C_{28}H_{14}$ (Table 2).

Key distances in C_{70} were also checked to determine if the interaction had an effect on the structure of C_{70} as well (Figure 22). The first, A, is the distance along the major axis from the centroid of each five-membered ring to the centroid of the C_{70}

molecule. The second, B, is the distance along the major axis between the centroids of the two five-membered rings. The last distance, C, is measured along the minor axis and is the average distance of the equatorial six-membered rings' centroid to the centroid of C_{70} . Comparison of the C_{70} distances in **2** to the distances of $C_{70} \cdot \{2,3,6,8,11,12,15,17\}$ -octamethyldibenzo-[b,i]1,4,8,11-tetraaza(1,4)annulene} nickel(II), Ni(OMTAA), and $\{C_{70} \cdot C_9C_{16}Br_3N\}$ present the idea that the C–C bonds of C_{70} were affected very little by the interactions with $C_{28}H_{14}$ (Table 3).^{48, 49}

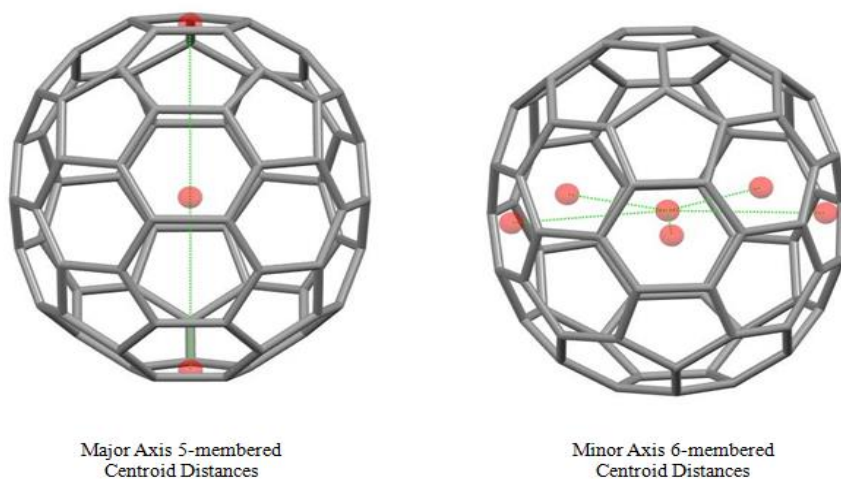


Figure 22. Depiction of distances **A**, **B**, and **C** in C_{70} .

Table 3. Key distances along the major and minor axes of C₇₀.

Centroid Distances (Å)	2	C ₇₀ ·Ni(OMTAA) ⁴⁸	C ₇₀ ·C ₉ Cl ₆ Br ₃ N ⁴⁹
A	3.950, 3.955	3.924, 3.950	3.961, 3.965
B	7.905	7.874	7.926
C	3.330	3.326	3.330

After expanding the asymmetrical unit in two directions, interactions between the adjacent C₂₈H₁₄ bowls as well as between C₇₀ with an C₂₈H₁₄ molecule creating a 1D strand have been identified. The C₂₈H₁₄ molecules along the strand interact through concave-convex C–H··· π interactions in which the distances alternate between 2.87 Å and 2.83 Å. The opposite end of the concave face of C₂₈H₁₄ is what binds to an adjacent C₇₀ molecule with C–H··· π interactions at alternating distances of 2.89 Å and 2.85 Å (Figure 23).

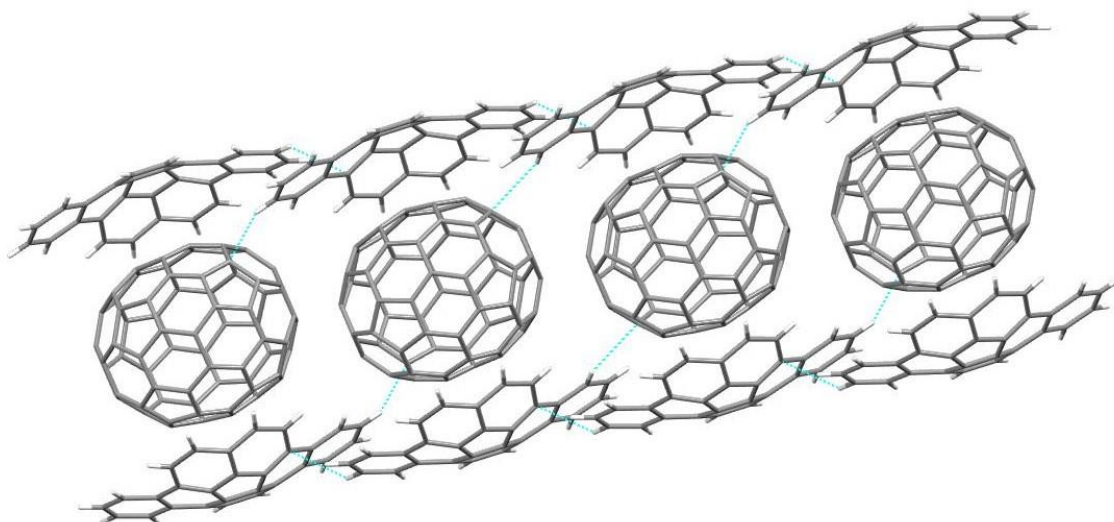


Figure 23. 1D stacking of **2** with DCB molecules omitted for clarity.

In addition, DCB molecules interact with the convex side of each $\text{C}_{28}\text{H}_{14}$ molecule through $\pi\cdots\pi$ interactions, with the shortest distance measured at 3.268(1) Å. Each DCB molecule interacts differently with the two adjacent $\text{C}_{28}\text{H}_{14}$ bowls; on one side it interacts with the hub bond of $\text{C}_{28}\text{H}_{14}$ and the other interacts with the rim bond attached to the a peripheral ring. Through these interactions multiple strands come together to form a 2D network of $\text{C}_{28}\text{H}_{14}$, C_{70} , and DCB (Figure 24).

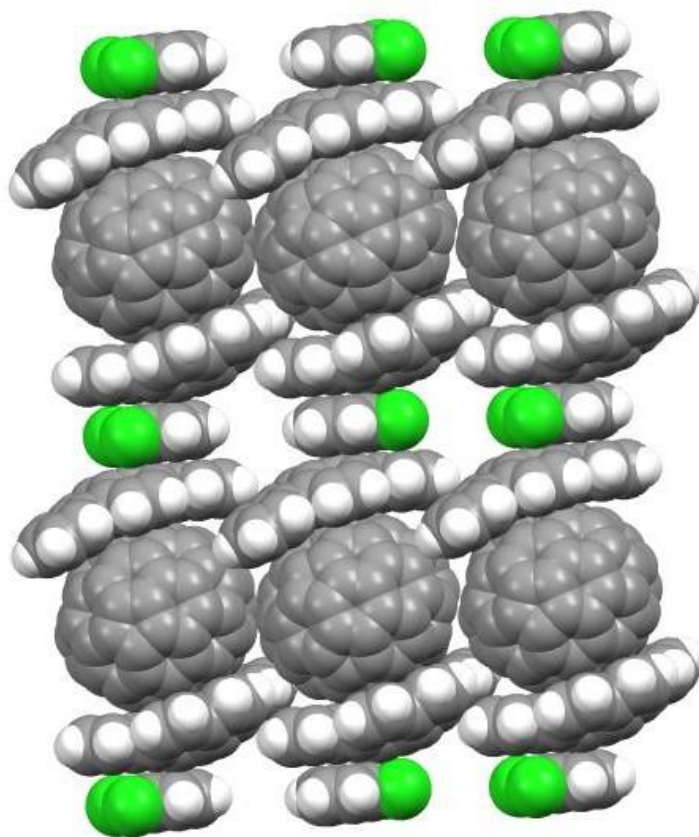


Figure 24. 2D stacking in **2**.

Unlike the adduct with C₆₀, a 3D packing structure is not observed for **2**. In this case, the sheets seem to be loosely held together through C–Cl \cdots π interactions with DCB molecules surrounding the C₇₀ molecules.

4.2 Characterization of Dibenzo[a,g]corannulene Anions

4.2.1 Rb Salt of C₂₈H₁₄ Monoanion

Single crystals of [Rb(18-crown-6)]⁺[C₂₈H₁₄][−], **3**, were grown from the DME solution of the monoreduced polyarene by layering with hexanes. The X-ray diffraction study of **3** revealed the formation of a contact-ion pair built on the symmetric central η^5 -binding of the Rb⁺ ion to the *exo* surface of the dibenzocorannulene core (Figure 25). Notably, in the contact-ion pair complexes of rubidium with monoreduced corannulene (C₂₀H₁₀[−]), a preferential convex metal binding was seen at the benzene ring site (*exo* η^6).

32

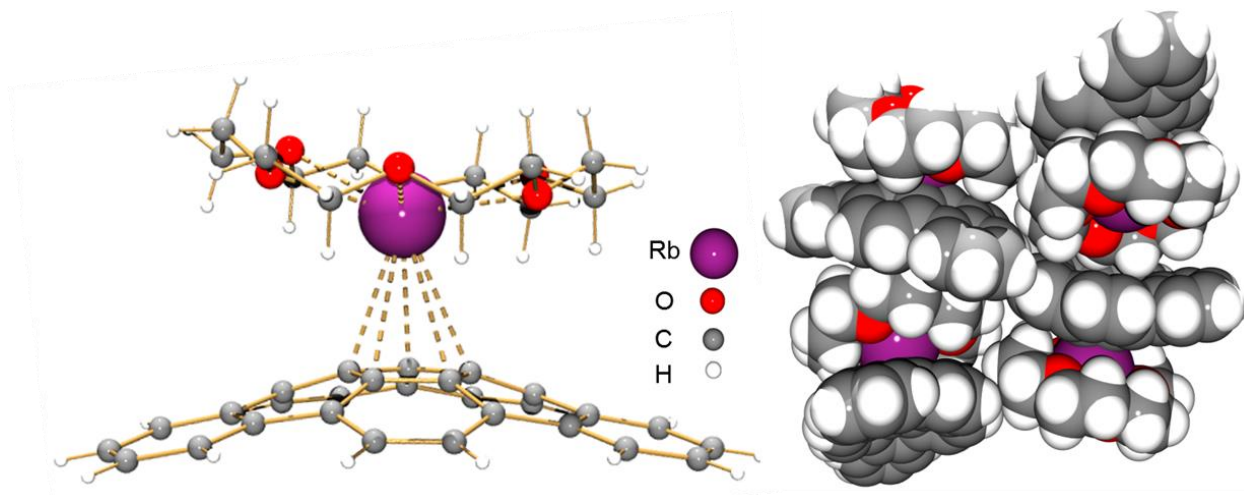


Figure 25. Molecular structure (left) and solid-state packing (right) of **3**.

The [Rb(18-crown-6)]⁺ cation sits almost exactly above the center of the five-membered ring. The Rb \cdots C_{hub} and Rb \cdots C_{centroid} bond lengths separations (3.161–3.326

and 3.018 Å, respectively) are indicative of the strong binding of the metal to the π -bowl. Notably, the Rb \cdots C distances in **3** are slightly shortened compared to those observed in the rubidium salt with corannulene monoanions.³³ The Rb⁺ ion is also bound to six oxygen atoms of the 18-crown-6 ether with the corresponding Rb \cdots O bond length distances (2.806(9)–2.989(10) Å) being close to those previously reported.^{33,50}

Moreover, interactions between the Rb⁺ ions with the peripheral rings of the neighboring C₂₈H₁₄^{•−} moieties were also observed in the crystal lattice of **3** (3.334 Å, Figure 26).

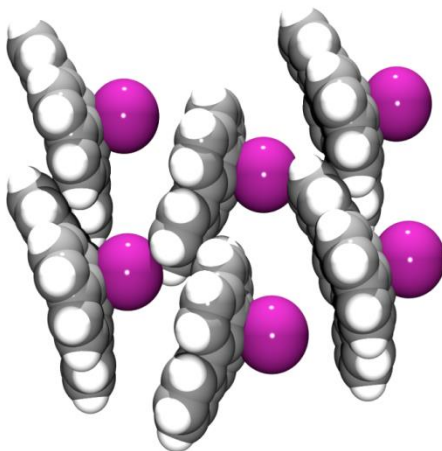


Figure 26. Space filling depiction of **3**. 18-crown-6 molecules have been removed for clarity.

The first structural characterization of C₂₈H₁₄^{•−} allows us to analyze the core perturbations in comparison to the parent bowl.⁴⁶ The spoke C–C bonds (av. 1.390(4) Å) are slightly elongated in **3** vs. those in neutral dibenzocorannulene (av. 1.372(2) Å).⁴³ The average hub and flank C–C bond distances are essentially the same in C₂₈H₁₄^{•−} and C₂₈H₁₄ (1.410(4) Å and 1.446(4) Å vs. 1.418(2) Å and 1.453(2) Å, respectively) (Table

4). The acquisition of one electron by dibenzocorannulene does not result in noticeable flattening of the corannulene core of the bowl (0.77 Å vs. 0.83 Å in the neutral ligand).

In the solid state structure, relatively short C–H $\cdots\pi$ separations are found between the 18-crown-6 molecules and adjacent C₂₈H₁₄^{•−} bowls (2.711(2)–2.877(2) Å, Figure 25). It is worth mentioning that several C–C contacts between two adjacent dibenzocorannulene bowls fall in the range 3.245(2)–3.370(2) Å (Figure 26). These values are shorter than the shortest C–C distances found in neutral C₂₈H₁₄ (3.34–3.60 Å).⁴⁶

Table 4. Ranges for key distances for C₂₈H₁₄, **3**, and **4** (in Å).

	C ₂₈ H ₁₄ ⁴⁶	3	4 *
hub	1.4208(2)–1.428(2)	1.400(4)–1.427(4)	1.393(3)–1.438(3) 1.392(3)–1.431(3)
rim	1.385(2)–1.447(2)	1.407(4)–1.456(4)	1.418(4)–1.471(4) 1.431(3)–1.466(3)
spoke	1.367(2)–1.380(2)	1.381(4)–1.398(4)	1.393(3)–1.415(3) 1.394(3)–1.417(4)
flank	1.435(2)–1.472(2)	1.412(4)–1.489(4)	1.408(4)–1.488(4) 1.402(3)–1.488(3)
peripheral rings	1.382(2)–1.407(2)	1.367(4)–1.416(4)	1.377(4)–1.417(3) 1.376(3)–1.415(3)
bowl depth	0.83	0.77	0.75 0.74

* Two crystallographically independent C₂₈H₁₄^{2−} anions with essentially close geometrical parameters have been observed in the unit cell.

4.2.2 Na Salt of C₂₈H₁₄ Dianion

Dark purple blocks of [Na(18-crown-6)(DME)⁺]₂[Na(18-crown-6)⁺][C₂₈H₁₄²⁻]₂, **4**, were grown by the slow diffusion of hexanes into the DME solution of doubly-reduced polyarene. According to an X-ray diffraction study, the [Na(18-crown-6)(DME)]₂⁺ and [Na(18-crown-6)]⁺ cations are solvent-separated from C₂₈H₁₄²⁻ anions (Figure 27), allowing the first structural evaluation of the “naked” C₂₈H₁₄²⁻ in which geometric parameters are not influenced by direct metal binding.

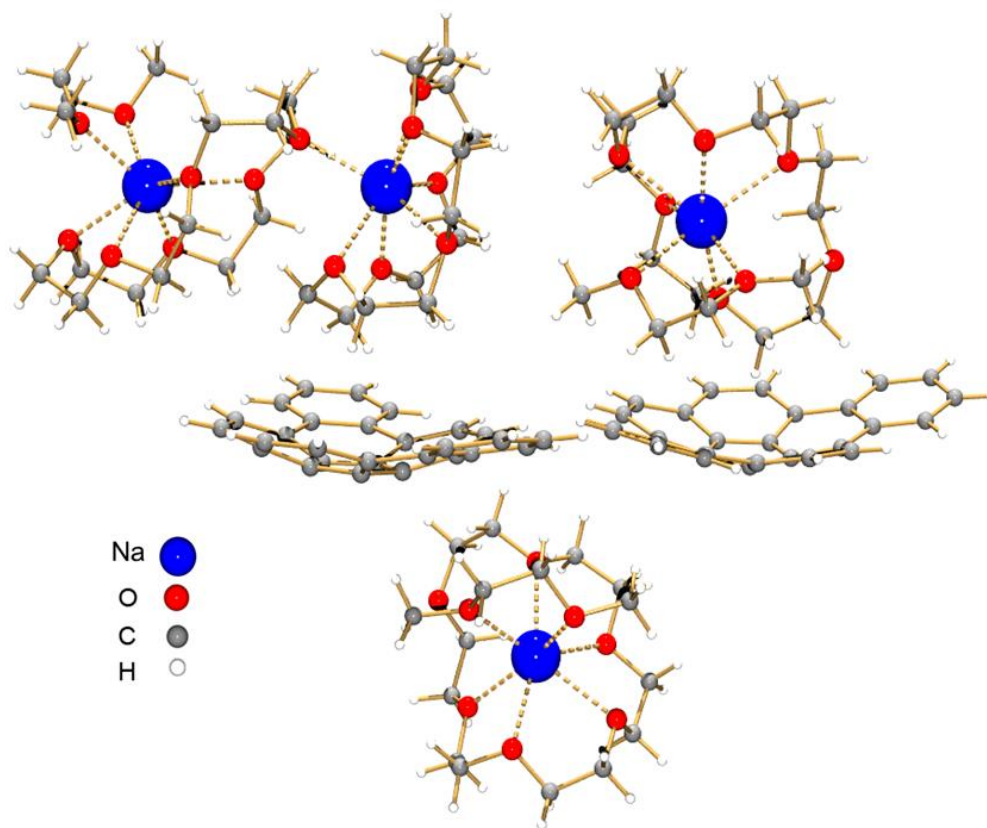


Figure 27. Molecular structure of **4**.

The sodium ion in [Na(18-crown-6)(DME)]₂⁺ is bound to one DME (2.341(2) and 2.472(2) Å) and one 18-crown-6 molecule (2.427(2)–2.798(2) Å). It is worth mentioning, the 18-crown-6 ether is bent and only five of its oxygen atoms are bound

to the Na⁺ ion. The Na⁺⋯O distances in the [Na(18-crown-6)(DME)]₂⁺ cation are longer than those in [Na(18-crown-6)]⁺ (2.365(2)–2.684(2) Å) having all six oxygen atoms coordinated to the Na⁺ cation.

In addition, the Na⁺ ion is bound to the oxygen atom of the adjacent 18-crown-6, in [Na(18-crown-6)(DME)]₂⁺, with the corresponding distance 2.380(2) Å. The observed full encapsulation of Na⁺ centers precludes any interactions between the alkali metal ions and π -surface of C₂₈H₁₄²⁻.

As shown in Table 4, the flank C–C bond lengths of C₂₈H₁₄²⁻ in **4** (av. 1.444(3) Å) are essentially the same as in C₂₈H₁₄ (av. 1.453(2) Å).⁴⁶ The average spoke and rim C–C bonds (1.440(3) Å and 1.400(3) Å, respectively) are slightly elongated *vs.* those in neutral dibenzocorannulene (1.372(2) Å and 1.418(2) Å, respectively). The acquisition of two electrons by dibenzocorannulene results in the flattening of the curved carbon surface compared to the neutral bowl (0.75 Å (av.) *vs.* 0.83 Å). At the same time, the bowl depth of C₂₈H₁₄²⁻ remains close to that in C₂₈H₁₄^{•-} (0.75 Å *vs.* 0.77 Å). For comparison, the addition of one and two electrons to C₂₀H₁₀ resulted in more pronounced changes (C₂₀H₁₀^{•-}: 0.834–0.855 Å and 0.785–0.811 Å, respectively *vs.* 0.875 Å in neutral C₂₀H₁₀).³⁸

In the solid state structure of **4**, both the concave and convex faces of C₂₈H₁₄²⁻ are involved in C–H⁺⋯ π interactions with the adjacent 18-crown-6 moieties. The shortest corresponding distances are 2.656 Å and 2.695 Å, respectively.

V. Experimental Part

5. Materials and Methods

Synthesis of dibenzo[*a,g*]corannulene was performed according to the established procedures, using the pathway stemming from the carbonylation of 2-chlorobenzyl chloride and diironnonacarbonyl.³⁸ The crude product was then purified further by washing it with hexanes followed by acetone. C₆₀ was purchased from TCI and C₇₀ was purchased from Sigma Aldrich; both were used as received. Anhydrous chlorobenzene and 1,2-dichlorobenzene was purchased from Sigma-Aldrich and degassed three times prior to use.

All manipulations were carried out using break-and-seal¹ and glove-box techniques under an atmosphere of argon. Solvents (THF, DME, and hexanes) were dried over Na/benzophenone and distilled prior to use. THF-*d*₈ was dried over NaK₂ alloy and vacuum-transferred. Crown ether, 18-crown-6 (99%), was purchased from Strem Chemicals and dried over P₂O₅ *in vacuo* for 24 h. Alkali metals were purchased from Strem Chemicals. Dibenzocorannulene was prepared as described previously and sublimed at 220 °C prior to use. The UV-vis spectra were recorded on a PerkinElmer Lambda 35 spectrometer. The ¹H NMR spectra were measured on a Bruker AC-400 spectrometer at 400 MHz and were referenced to the resonances of the corresponding solvent used. The X-ray intensity data for **1** were measured on a Bruker Kappa APEX DUO diffractometer equipped with a Cu INCOATEC ImS micro-focus source ($\lambda = 1.54178$ Å). The X-ray intensity data for **2** were measured on a Bruker D8 VENTURE with PHOTON 100 CMOS detector system equipped with a Cu INCOATEC ImS micro-focus source ($\lambda = 1.54178$ Å). Data collection of **3** and **4** were performed on a Bruker

SMART APEX CCD-based X-ray diffractometer with graphite-monochromated Mo K α radiation ($\lambda = 0.71073 \text{ \AA}$).

5.1 Preparation of [C₆₀·C₂₈H₁₄] (1) and [(C₇₀)(C₂₈H₁₄)₂]·3C₆H₄Cl₂ (2).

To form **1**, dibenzocorannulene (3.0 mg, 0.009 mmol) and C₆₀ (6.18 mg, 0.009 mmol) were dissolved in chlorobenzene (2.2 mL). The purple solution was filtered into a “L-shaped” ampoule (shown below), degassed three times, and sealed under vacuum. The ampoule was slightly tilted and the end without any solution was placed into an ice bath. The ice was placed in an insulated container and replenished when necessary (Figure 28). Crystals were present in low yield in 120 hours. The solution was decanted away from the crystals, and the crystals were sealed under vacuum.

Synthesis of crystals of **2** followed the same procedure, substituting C₇₀ (7.2 mg, 0.009 mmol) in place of C₆₀ and 1,2-dichlorobenzene (2.2 mL) for chlorobenzene.

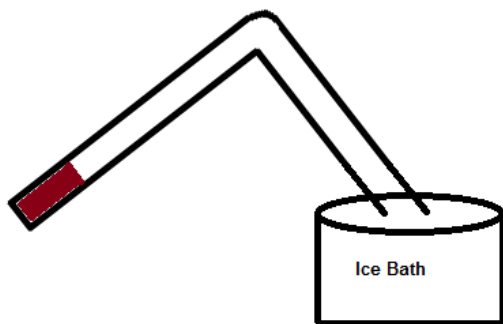


Figure 28. Depiction of the slow evaporation using a sealed “L-shaped” ampoule and ice bath.

5.2 Preparation of [Rb(18-crown-6)⁺][C₂₈H₁₄[−]] (3)

DME (3 mL) was added to a flask containing Rb metal (3.6 mg, 0.042 mmol, 1.5 eq.), dibenzocorannulene (10 mg, 0.0286 mmol), and 18-crown-6 (8 mg, 0.0286 mmol). The resulting deep green-blue solution was stirred at room temperature for 5 hours. The blue-green mixture was filtered, layered with hexanes (3 mL) and kept at 10 °C. Green crystals (blocks) were present in 48 hours. The green solution was decanted, and the crystals were washed several times with hexanes and dried *in vacuo*. Yield: 17 mg, 85%. Uv-vis (THF, nm): 469, 656 (Figure 29). ¹H NMR (400 MHz, THF-*d*₈, 15 mM, 25 °C, ppm): δ = 3.25, 3.42; ¹H NMR (400 MHz, THF-*d*₈, 15 mM, −60 °C, ppm): δ = 3.25, 3.42.

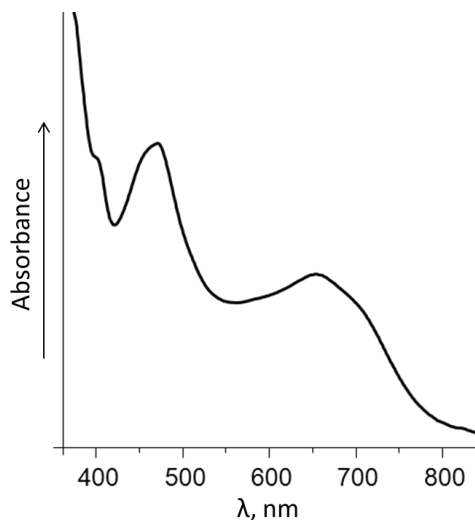


Figure 29. Uv-vis spectrum of **3** (THF).

5.3 Preparation of $[\text{Na}(\text{18-crown-6})(\text{DME})^+]_2[\text{Na}_2(\text{18-crown-6})_2(\text{DME})^{2+}][\text{C}_{28}\text{H}_{14}^{2-}]_2$ (**4**)

DME (3 mL) was added to a flask containing excess Na metal, dibenzocorannulene (10 mg, 0.0286 mmol), and 18-crown-6 (8 mg, 0.0286 mmol). The deep green solution was stirred at room temperature for 8 hours resulting in a deep purple mixture. The purple mixture was filtered, layered with hexanes (3 mL) and kept at 10 °C. Purple crystals (blocks) were present in 36 hours. The solution was decanted, and the crystals were washed several times with hexanes and dried *in vacuo*. Yield: 45 mg, 70%. UV-vis (THF, nm): $\lambda_{\text{max}} = 544, 655$ (Figure 30).

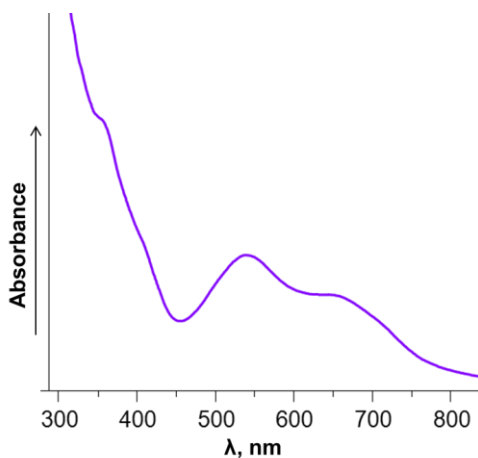


Figure 30. UV-vis spectrum of **4** (THF).

VI. Conclusions

With the preparation of $[\text{C}_{60}\cdot\text{C}_{28}\text{H}_{14}]$ (**1**) and $[(\text{C}_{70})(\text{C}_{28}\text{H}_{14})_2]\cdot 3\text{C}_6\text{H}_4\text{Cl}_2$ (**2**), we have produced the first two examples of co-crystallization of dibenzo[*a,g*]corannulene with fullerenes. Upon analysis of each crystal structure, a remarkable difference was noticed between the two packing patterns. Adduct **1** exhibits packing similar to that of $\text{C}_{60}\cdot\text{C}_{20}\text{H}_{10}$ in which a 1:1 ratio of fullerene:buckybowl has been previously observed with a lack of differentiation between concave-convex and convex-convex binding. The structure of **2** exhibits a completely different and unique packing motif. In this assembly, two $\text{C}_{28}\text{H}_{14}$ molecules interact with C_{70} only through concave-convex interactions, essentially encapsulating each C_{70} molecule by two bowls in the crystal. Also unique to this self-assembly, $\text{C}_{28}\text{H}_{14}$ exclusively interacts with the elongated major axis of C_{70} , suggesting a preferential binding mode between these two molecules. Future applications of these interactions may include using dibenzo[*a,g*]corannulene as the receptors in a pair of “molecular tweezers” to selectively capture the C_{70} guest molecules in the presence of C_{60} .

With the preparation of crystals of $[\text{Rb}(18\text{-crown-6})^+][\text{C}_{28}\text{H}_{14}^-]$ (**3**) and $[\text{Na}(18\text{-crown-6})(\text{DME})^+]_2[\text{Na}_2(18\text{-crown-6})_2(\text{DME})^{2+}][\text{C}_{28}\text{H}_{14}^{2-}]_2$ (**4**), we have characterized the first mono and dianion of dibenzo[*a,g*]corannulene. The single crystal X-ray diffraction study of **3** revealed the presence of a contact-ion pair for the monoanion, with the preferential metal binding to the *exo* face of $\text{C}_{28}\text{H}_{14}^-$. The structural analysis of **4** demonstrated the presence of a “naked” dianion of $\text{C}_{28}\text{H}_{14}$. In each of these anions, the bowl depth of $\text{C}_{28}\text{H}_{14}$ showed a negligible change upon addition of electrons as compared

to neutral $\text{C}_{28}\text{H}_{14}$. Successful isolation of these anions provides a solid foundation toward future use of dibenzo[*a,g*]corannulene in electron storing materials.

VII. References

- ¹ (a) Matsuo, Y.; Nakamura, E. Application of Fullerenes to Nanodevices. In *Chemistry of Nanocarbons*; Akasaka, T.; Wudl, F.; Nagase, S. Eds., John Wiley & Sons, Ltd: Chichester, 2010, 173–187; (b) Rodríguez-Fortea, A.; Balch, A. L.; Poblet, J. M., Endohedral metallofullerenes: a unique host-guest association. *Chem. Soc. Rev.* **2011**, *40*, 3551–3563; (c) Lu, X.; Akasaka, T.; Nagase, S., Chemistry of endohedral metallofullerenes: the role of metals. *Chem. Commun.* **2011**, *47*, 5942–5957.
- ² Pinzón, J. R.; Villalta-Cerdas, A.; Echegoyen, L., Fullerenes, Carbon Nanotubes, and Graphene for Molecular Electronics. *Unimolecular and Supramolecular Electronics I*, Metzger, R. M. Eds.; Topics in Current Chemistry; Springer Berlin Heidelberg, **2012**, *312*, 127–174.
- ³ Chamberlain, T. W.; Meyer, J. C.; Biskupek, J.; Leschner, J.; Santana, A.; Besley, N. A.; Bichoutskaia, E.; Kaiser, U.; Khlobystov, A. N., Reactions of the inner surface of carbon nanotubes and nanoprotrusion processes imaged at the atomic scale. *Nat. Chem.* **2011**, *3*, 732–737.
- ⁴ Haddon R. C.; Brus, L. E.; Raghavachari, K., Electronic Structure and Bonding in Icosahedral Carbon Cluster (C₆₀). *Chem. Phys. Lett.* **1986**, *125*, 459–464.
- ⁵ *Carbon-Rich Compounds: From Molecules to Materials*; Kitagawa, T.; Toshikazu, M.; Yasurjiro, K. K; Eds. Haley, M. M.; Tykwinski, R. R.; Wiley-VCH Verlag GmbH & Co. KGaA, **2006**, pg. 383–420.

-
- ⁶ Kroto, H. W.; Heath, J. R.; O'Brien, S. C.; Curl, R. F.; Smalley, R. E., C₆₀: Buckminsterfullerene. *Nature* **1985**, *318*, 162–163.
- ⁷ Bachawala, P. Large Scale Synthesis and Derivatization of Corannulene - The Smallest Buckybowl. Mississippi State University, 2006.
- ⁸ Arie, A. A.; Lee, J. K., Nano-Carbon Coating Layer Prepared by the Thermal Evaporation of Fullerene C₆₀ for Lithium Metal Anodes in Rechargeable Lithium Batteries. *J. Nanosci. Nanotechnol.* **2011**, *11*, 6569–6574.
- ⁹ Scott, L. T., Fragments of Fullerenes: Novel Syntheses, Structures and Reactions. *Pure & Appl. Chem.* **1996**, *68*, 291–300.
- ¹⁰ Petrukhina, M. A.; Scott, L. T., Coordination Chemistry of Buckybowls: From Corannulene to a Hemifullerene. *Dalton Trans.* **2005**, 2969–2975.
- ¹¹ Wu, Y. T.; Siegel, J. S., Aromatic Molecular-Bowl Hydrocarbons: Synthetic Derivatives, Their Structures, and Physical Properties. *Chem. Rev.* **2006**, *106*, 4843–4867.
- ¹² Barth, W. E.; Lawton, R. G., Dibenzo[ghi,mno]fluoranthene. *J. Am. Chem. Soc.* **1966**, *88*, 380–381.
- ¹³ Janata, J.; Gendell, J.; Ling, C.-Y.; Barth, W.; Backs, L.; Mark Jr., H. B.; Lawton, R. G., Concerning the Anion and Cation Radicals of Corannulene. *J. Am. Chem. Soc.* **1967**, *89*, 3056–3058.
- ¹⁴ Sygula, A.; Rabideau, P. W., Non-Pyrolytic Syntheses of Buckybowls: Corannulene, Cyclopentacorannulene, and a Semibuckminsterfullerene. *J. Am. Chem. Soc.* **1999**, *121*, 7800–7803.

-
- ¹⁵ Scott, L. T.; Hashemi, M. M.; Meyer, D. T.; Warren, H. B., Corannulene. A Convenient New Synthesis. *J. Am. Chem. Soc.* **1991**, *113*, 7082–7084.
- ¹⁶ Hanson, J. C.; Nordman, C. E., The Crystal and Molecular Structure of Corannulene (C₂₀H₁₀). *Acta Crystallogr.* **1976**, *B32*, 1147–1153; (b) Petrukhina, M.A.; Andreini, K. W.; Mack, J.; Scott, L. T., X-ray Quality Geometries of Geodesic Polyarenes from Theoretical Calculations: What Levels of Theory Are Reliable? *J. Org. Chem.* **2005**, *70*, 5713–5716.
- ¹⁷ Steiner, E.; Fowler, P. W., Jenneskens, L. W., Counter-Rotating Ring Currents in Coronene and Corannulene. *Angew. Chem. Int. Ed.* **2001**, *40*, 362–366.
- ¹⁸ (a) Ayalon, A.; Rabinovitz, M.; Cheng, P.-C.; Scott, L. T., The Corannulene Tetraanion: A Novel Species with Concentric Aromatic Rings. *Angew. Chem. Int. Ed. Engl.* **1992**, *31*, 1636–1637 (b) Ayalon, A.; Sygula, A.; Cheng, P.-C.; Rabinovitz, M.; Rabideau, P. W.; Scott, L. T., Stable High-Order Molecular Sandwiches: Hydrocarbon Polyanion Pairs with Multiple Lithium Ions Inside and Out. *Science* **1994**, *265*, 1065–1067; (c) Shenhar, R.; Willner, I.; Preda, D. V.; Scott, L. T.; Rabinovitz, M., Electron Photoejection from Corannulene Dianion and Li⁺-Mediated Recombination of the Photogenerated Species. *J. Phys. Chem. A* **2000**, *104*, 10631–10636; (d) Shabtai, E.; Hoffman, R. E.; Cheng, P.-C.; Bayrd, E.; Preda, D. V.; Scott, L. T.; Rabinovitz, M., Reduced Corannulenes: 1,8-dicorannuleneyloctane Anions, A Supramolecular Octaanion. *J. Chem. Soc. Perkin Trans. 2* **2000**, 129–133; (e) Aprahamian, I.; Eisenberg, D.; Hoffman, R. E.; Sternfeld, T.; Matsuo, Y.; Jackson, E. A.; Nakamura, E.; Scott, L. T.; Sheradsky, T.; Rabinovitz, M., Ball-and-Socket Stacking of Supercharged Geodesic

Polyarenes: Bonding by Interstitial Lithium Ions. *J. Am. Chem. Soc.* **2005**, *127*, 9581–9587.

¹⁹ Filatov, A. S.; Bowl-shaped Polyaromatic Hydrocarbons (Buckybowls): Crystal Packing and Metal Binding Reactions. University at Albany, 2009.

²⁰ Denis, P. A., Theoretical Investigation of the Stacking Interactions Between Curved Conjugated Systems and their Interaction with Fullerenes. *Chem. Phys. Lett.* **2011**, *516*, 82–87; (b) Muck-Lichtenfeld, C.; Grimme, S.; Kobryn, L.; Sygula, A., Inclusion Complexes of Buckycatcher with C₆₀ and C₇₀. *Phys. Chem. Chem. Phys.*, **2010**, *12*, 7091–7097; (c) Jackson, E. A.; Steinberg, B. D.; Bancu, M.; Wakamiya A.; Scott, L. T., Pentaindenocorannulene and Tetraidenocorannulene: New Aromatic Hydrocarbon π Systems with Curvatures Surpassing that of C₆₀. *J. Am. Chem. Soc.* **2006**, *129*, 484–485.

²¹ Dawe, L. N.; Al Hujran, T. A.; Tran, H.-A.; Mercer, J. I.; Jackson, E. A.; Scott, L. T.; Georghiou, P. E., Corannulene and its Penta-tert-butyl Derivative Co-crystallize 1:1 with Pristine C₆₀-Fullerene. *Chem. Commun.* **2012**, *48*, 5563–5565.

²² (a) Makha, M.; Purich, A.; Raston, C. L.; Sobolev, A. N. Structural Diversity of Host-guest and Intercalation Complexes of Fullerene C₆₀. *Eur. J. Inorg. Chem.* **2006**, 507–517; (b) Franco, J. U.; Hammons, J. C.; Rios, D.; Olmstead, M. M., New Tetraazaannulene Hosts for Fullerenes. *Inorg. Chem.* **2010**, *49*, 5120–5125.

²³ Sygula, A.; Fronczek, F. R.; Sygula, R.; Rabideau, P. W.; Olmstead, M. M., A Double Concave Hydrocarbon Buckycatcher. *J. Am. Chem. Soc.* **2007**, *129*, 3842–3843.

-
- ²⁴ Filatov, A. S.; Petrukhina, M. A., Probing the Binding Sites and Coordination Limits of Buckybowls in a Solvent-Free Environment: Experimental and Theoretical Assessment. *Coord. Chem. Rev.* **2010**, *254*, 2234–2246.
- ²⁵ Petrukhina, M. A., Coordination of Buckybowls: The First Concave-Bound Metal Complex. *Angew. Chem. Int. Ed.* **2008** *47*, 1550–1552.
- ²⁶ Zhu, B; Ellern, A; Sygula, A; Sygula, R; Angelici, R. J., η^6 -Coordination of the Curved Carbon Surface of Corannulene (C₂₀H₁₀) to (η^6 -arene) M²⁺ (M = Ru, Os) *Organometallics* **2007**, *26*, 1721–1728.
- ²⁷ Petrukhina, M. A.; Andreini, K. W.; Mack, J.; Scott, L. T., Transition-metal Complexes of an Open Geodesic Polyarene. *Angew. Chem. Int. Ed.* **2003**, *42*, 3375–3379.
- ²⁸ Petrukhina, M. A.; Sevryugina, Y.; Rogachev, A. Y.; Jackson, E. A.; Scott, L. T.; Corannulene: A Preference for *exo*-Metal Binding. X-ray Structural Characterization of [Ru₂(O₂CCF₃)₂(CO)₄•(η -C₂₀H₁₀)₂]. *Organometallics*. **2006**, *25*, 5492–5495.
- ²⁹ Petrukhina, M.A.; Sevryugina, Y.; Rogachev, A. Y.; Jackson, E. A.; Scott, L.T., Corannulene “Hub” Carbon Coordination by [Ru₂{O₂C(3,5-CF₃)₂C₆H₃}₂(CO)₅]. *Angew. Chem. Int. Ed.* **2006**, *45*, 7208–7210.
- ³⁰ Elliott, E. L.; Hernández, G. A.; Linden, A.; Siegel, J. S., Anion Mediated Structural Motifs in Silver(I) Complexes with Corannulene. *Org. Biomol. Chem.* **2005**, *3*, 407–413.
- ³¹ Vecchi, P. A.; Albarez, C. M.; Ellern, A.; Angelici, R. J.; Sygula, A.; Sygula, R.; Rabideau, P. W., Synthesis and Structure of a Dimetallated Buckybowl: Coordination of One {Cp*Ru}⁺ Unit to Each Side of Corannulene. *Angew. Chem. Int. Ed.*, **2004**, *43*, 4497–4500.

-
- ³² Siegel, J. S.; Baldrige, K. K.; Linden, A.; Dorta, R., D8 Rhodium and Iridium Complexes of Corannulene. *J. Am. Chem. Soc.* **2006**, 128, 10644–10645.
- ³³ Spisak, S. N.; Zabula, A. V.; Filatov, A. S.; Rogachev, A. Yu.; Petrukhina, M. A., Selective Endo and Exo Binding of Alkali Metals to Corannulene. *Angew. Chem. Int. Ed.* **2011**, 50, 8090–8094.
- ³⁴ Baumgarten, M.; Gherghel, J. L.; Wagner, M.; Weitz, A.; Rabinovitz, M.; Cheng, P.-C.; Scott, L. T., Corannulene Reduction: Spectroscopic Detection of All Anionic Oxidation States. *J. Am. Chem. Soc.* **1995**, 117, 6254–6257.
- ³⁵ Spisak, S. N.; Zabula, A. V.; Filatov, A. S.; Petrukhina, M. A., unpublished results.
- ³⁶ Zabula, A. V.; Spisak, S. N.; Filatov, A. S.; Petrukhina, M. A., Self-Assembly of Charged Supramolecular Sandwiches Formed by Corannulene Tetraanions and Lithium Cations. *Organometallics*. **2012**, 31, 5541–5545.
- ³⁷ Zabula, A. V.; Filatov, A. S.; Spisak, S. N.; Rogachev, A. Y.; Petrukhina, M. A., A Main Group Metal Sandwich: Five Lithium Cations Jammed Between Two Corannulene Tetraanion Decks. *Science*. **2011**, 333, 1008–1011.
- ³⁸ (a) Zabula, A. V.; Spisak, S. N.; Filatov, A. S.; Grigoryants, V. M.; Petrukhina, M. A., How Charging Corannulene with One and Two Electrons Affects Its Geometry and Aggregation with Sodium and Potassium Cations. *Chem.–Eur. J.* **2012**, 18, 6476–6484;
(b) Spisak, S. N.; Zabula, A. V.; Ferguson, M. V.; Filatov, A. S.; Petrukhina, M. A., “Naked” Mono- and Dianions of Corannulene with Lithium Counterions. *Organometallics* **2013**, 32, 538–543.
- ³⁹ Spisak, S. N.; Zabula, A. V.; Filatov, A. S.; Petrukhina, M. A., unpublished results.

-
- ⁴⁰ Bruno, C.; Benassi, R.; Passalacqua, A.; Paolucci, F.; Fontanesi, C.; Marcaccio, M.; Jackson, E. A.; Scott, L. T., Electrochemical and Theoretical Investigation of Corannulene Reduction Process. *J. Phys. Chem. B.* **2009**, *113*, 1954–1962.
- ⁴¹ Tsefrikas, V. M., Ph.D. Dissertation, Boston College, Chestnut Hill, MA 2007.
- ⁴² Sun, X.; Zhao, W., Prediction of Stiffness and Strength of Single-Walled Carbon Nanotubes by Molecular-Mechanics Based Finite Element Approach. *Mater. Sci. Eng., A* **2005**, *390*, 336–371.
- ⁴³ Scott, L. T.; Jackson, E. A.; Zhang, Q.; Steinberg, B. D.; Bancu, M.; Li, Bo., A Short, Rigid, Structurally Pure Carbon Nanotube by Stepwise Chemical Synthesis. *J. Am. Chem. Soc.* **2012**, *134*, 107–110.
- ⁴⁴ Bratcher, M. S. Ph.D. Dissertation, Boston College, Chestnut Hill, MA 1996.
- ⁴⁵ Reisch, H. A.; Bratcher, M. S.; Scott, L. T., Imposing Curvature on a Polyarene by Intramolecular Palladium-Catalyzed Arylation Reactions: A Simple Synthesis of Dibenzo[*a,g*]corannulene. *Org. Lett.* **2000**, *2*, 1427–1430.
- ⁴⁶ Petrukhina, M. A.; Andreini, K. W.; Tsefrikas, V. M.; Scott, L. T., Unprecedented Complexation of Two Transition Metals to the Concave Surface of Geodesic Polyarene: {[Rh₂(O₂CCF₃)₄]₃(dibenzo[*a,g*]corannulene)₂}. *Organometallics* **2005**, *24*, 1394–1397.
- ⁴⁷ (a) Weitz, A.; Shabtai, E.; Rabinovitz, M.; Bratcher, M. S.; McComas, C. C.; Best, M. D.; Scott, L. T., Dianions and Tetraanions of Bowl-Shaped Fullerene Fragments Dibenzo[*a,g*]corannulene and Dibenzo[*a,g*]cyclopenta[*kl*]corannulene. *Chem.–Eur. J.* **1998**, *4*, 234–239; (b) Benshafrut, R.; Shabtai, E.; Rabinovitz, M.; Scott, L. T., π -Conjugated Anions: From Carbon-Rich Anions to Charged Carbon Allotropes. *Eur. J.*

Org. Chem. **2000**, 1091–1106; (c) *Fragments of Fullerenes and Carbon Nanotubes: Designed Synthesis, Unusual Reactions, and Coordination Chemistry*; Petrukhina, M. A.; Scott, L. T. Eds.; John Wiley & Sons: New Jersey, 2012, pg. 63–93.

⁴⁸ Croucher, P. D.; Marshall, J. M. E.; Nichols, P. J.; Raston, C. L., Confinement of C₇₀ in an Extended Saddle Shaped Nickel(II) Macrocyclic. *Chem Comm.* **1999**, 193–194.

⁴⁹ Pham, D.; Ceron-Bertran, J.; Olmstead, M. M.; Mascal, M.; Balch, A. L., Ordered Crystals of Fullerenes Produced by Cocrystallization with Halogenated Azatriquinacenes. *Crystal Growth & Design.* **2007**, 7, 75–82.

⁵⁰ (a) Boeddinghaus, M. B.; Salzinger, M.; Fässler, T. F., Synthesis, X-ray Single-Crystal Structure Determination, and Magnetic Properties of [Rb(benzo[18]crown-6)]⁺ Salts Containing Well-Ordered Fulleride Trianions C₆₀³⁻. *Chem.–Eur. J.* **2009**, 15, 3261–3267.